

See discussions, stats, and author profiles for this publication at: <https://www.researchgate.net/publication/231270076>

Chemical percolation model for devolatilization. 3. Direct use of ^{13}C NMR data to predict effects of coal type

ARTICLE in ENERGY & FUELS · JULY 1992

Impact Factor: 2.79 · DOI: 10.1021/ef00034a011

CITATIONS

152

READS

3,933

5 AUTHORS, INCLUDING:



Thomas H. Fletcher

Brigham Young University - Provo Main Campus

155 PUBLICATIONS 2,299 CITATIONS

SEE PROFILE



Alan R. Kerstein

Stochastic Sciences

199 PUBLICATIONS 4,463 CITATIONS

SEE PROFILE



Ronald Pugmire

University of Utah

266 PUBLICATIONS 6,305 CITATIONS

SEE PROFILE



Mark S. Solum

University of Utah

71 PUBLICATIONS 1,978 CITATIONS

SEE PROFILE

Chemical Percolation Model for Devolatilization. 3. Direct Use of ^{13}C NMR Data To Predict Effects of Coal Type

Thomas H. Fletcher* and Alan R. Kerstein

Combustion Research Facility, Sandia National Laboratories,
Livermore, California 94551-0969

Ronald J. Pugmire,[†] Mark S. Solum,[‡] and David M. Grant[†]

Departments of Fuels Engineering and Chemistry, University of Utah,
Salt Lake City, Utah 84112

Received March 16, 1992. Revised Manuscript Received May 6, 1992

The chemical percolation devolatilization (CPD) model describes the devolatilization behavior of rapidly heated coal based on the chemical structure of the parent coal. Percolation lattice statistics are employed to describe the generation of tar precursors of finite size based on the number of cleaved labile bonds in the infinite coal lattice. The chemical percolation devolatilization model described here includes treatment of vapor-liquid equilibrium and a cross-linking mechanism. The cross-linking mechanism permits reattachment of metaplast to the infinite char matrix. A generalized vapor pressure correlation for high molecular weight hydrocarbons, such as coal tar, is proposed based on data from coal liquids. Coal-independent kinetic parameters are employed. Coal-dependent chemical structure coefficients for the CPD model are taken directly from ^{13}C NMR measurements, with the exception of one empirical parameter representing the population of char bridges in the parent coal. This is in contrast to the previous and common practice of adjusting input coefficients to precisely match measured tar and total volatiles yields. The CPD model successfully predicts the effects of pressure on tar and total volatiles yields observed in heated grid experiments for both bituminous coal and for lignite. Predictions of the amount and characteristics of gas and tar from many different coals compare well with available data, which is unique because the majority of model input coefficients are taken directly from NMR data and are not used as empirical fitting coefficients. Predicted tar molecular weights are consistent with size-exclusion chromatography (SEC) data and field ionization mass spectrometry (FIMS) data. Predictions of average molecular weights of aromatic clusters as a function of coal type agree with corresponding data from NMR analyses of parent coals. The direct use of chemical structure data as a function of coal type helps justify the model on a mechanistic rather than an empirical basis.

Introduction

Coal is commonly thought to consist of a large (essentially infinite) matrix of clusters of fused aromatic rings connected by aliphatic bridges. Side chain attachments to the aromatic clusters include aliphatic ($-\text{CH}_n$) and carbonyl ($-\text{CO}_2$) groups, which are light gas precursors. A small fraction of the clusters in the parent coal are unattached to the infinite matrix and can be extracted using suitable solvents without breaking any bonds. Several hypothetical chemical structures for coal macromolecules have been suggested;¹⁻⁴ a simplistic approach is used in this work, with broad definitions of clusters, bridges, side chains, and loops, as illustrated in Figure 1. Coal pyrolysis products include light gases, tar (hydrocarbons that condense at room temperature and pressure), and char.

Models of coal devolatilization have progressed from simple empirical expressions of total mass release, involving one or two rate expressions, to more complex descriptions of the chemical and physical processes involved. The chemical and physical processes that occur during coal pyrolysis have been discussed at length by several investigators.^{3,5-9} During coal pyrolysis, the labile bonds between the aromatic clusters are cleaved, and fragments of

finite molecular weight are generated. The fragments with low molecular weights vaporize, due to their high vapor pressure, and escape from the coal particle as tar vapor. The fragments with high molecular weight, and hence low vapor pressures, remain in the coal at typical devolatilization conditions. These high molecular weight compounds are often referred to as metaplast; the quantity and nature of the metaplast generated during devolatilization determines the softening behavior of the particle.

The relationship between the number of labile bonds broken and the mass of finite fragments liberated from the infinite coal lattice is highly nonlinear, demonstrating that coal pyrolysis is not a simple vaporization process. Freihaut and Proscia¹⁰ collected coal tars from a heated screen

* Author to whom correspondence should be addressed. Presently at the Department of Chemical Engineering, 350 CB, Brigham Young University, Provo, Utah, 84602.

[†] Department of Fuels Engineering.

[‡] Department of Chemistry.

- (1) Given, P. H. *Fuel* 1960, 39, 147.
- (2) Wiser, W. H. In *Proceedings of the Electric Power Research Institute Conference on Coal Catalysis*; Palo Alto, CA, 1973; p 3.
- (3) Solomon, P. R.; Hamblen, D. G. In *Chemistry of Coal Conversion*; Schlosberg, R. H., Ed.; Plenum: New York, 1985; p 121.
- (4) Shinn, J. H. *Fuel* 1984, 63, 1187.
- (5) Howard, J. B. In *Chemistry of Coal Utilization*; Elliott, M. A., Ed.; Wiley: New York, 1981; p 665.
- (6) Gavalas, G. R. *Coal Pyrolysis*; Elsevier: Amsterdam, The Netherlands, 1981.
- (7) Suuberg, E. M. In *Chemistry of Coal Conversion*; Schlosberg, R. H., Ed.; Plenum: New York, 1985; p 67.
- (8) Serio, M. A.; Hamblen, D. G.; Markham, J. R.; Solomon, P. R. *Energy Fuels* 1987, 1, 138.
- (9) Grant, D. M.; Pugmire, R. J.; Fletcher, T. H.; Kerstein, A. R. *Energy Fuels* 1989, 3, 175.
- (10) Freihaut, J. D.; Proscia, W. M. Presented at the *Seventh Annual International Pittsburgh Coal Conference*; Pittsburgh, PA, Sep 10-14, 1990.

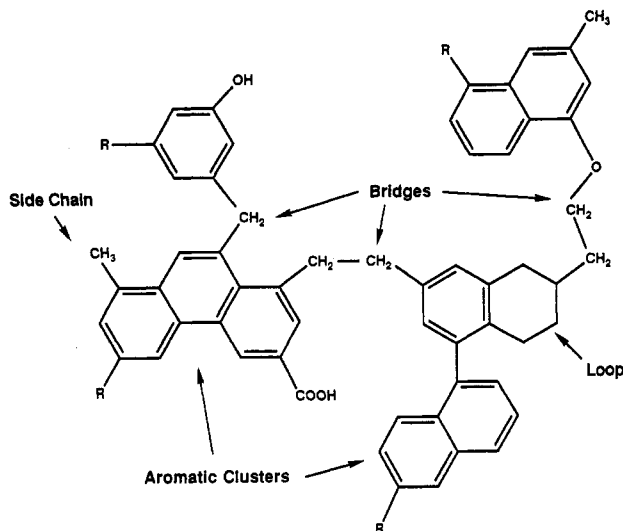


Figure 1. Representative chemical structures identified in ^{13}C NMR analyses and used in the description of coal and coal chars in the CPD model.

reactor and then measured the temperature at which these tars would revaporize in a subsequent experiment at identical heating conditions. The coal tars revaporized at significantly lower temperatures than the original temperature of tar release from the coal. These results show that coal pyrolysis is not just a vaporization process and suggest that lattice networks may be necessary to describe coal pyrolysis reactions.

Several devolatilization models have been developed in the last few years that treat the coal matrix as a lattice network in order to model tar formation and release. A chronology of the development of devolatilization models is given in some detail in an earlier paper⁹ and is only briefly reviewed here.

Solomon and co-workers¹¹ developed a devolatilization model (FG/DVC) that uses a Monte Carlo simulation to describe the breakup of an array of aromatic clusters connected by labile bridges. This model incorporates a set of 19 reactions, each with distributed activation energies, for the release of 12 light gases which are related to functional groups observed in the parent coal matrix. This model includes a scheme based on the vapor pressure of the metaplast to determine which finite fragments are released as tar. Cross-linking is also modeled based on empirical correlations with CO_2 release for lignites and CH_4 release for all other coals. The Monte Carlo method is somewhat time consuming and permits a great deal of subjectivity in the selection of the initial coal matrix.

Niksa and Kerstein¹² approximated the coal as a linear chain of aromatic clusters connected by labile bridges and used percolation statistics applied to straight chains to obtain a closed relationship between the number of broken bridges and the number of detached fragments. This model was recently extended to include a flash distillation mechanism¹³ to treat vapor-liquid equilibrium between tar and metaplast.¹⁴ This model (FLASHCHAIN) is also capable of treating cross-linking, and the authors discuss predictions performed with and without the cross-linking mechanism. However, it is well-known that coal molecules exhibit branching between clusters, and the chain structure underestimates the degree of connectivity in the macro-

molecular network. Attempts are made in FLASHCHAIN to use information regarding the coal structure as input parameters, such as the molecular weight per cluster. However, the coordination number (number of total attachments per cluster) is set to two, and all of the molecular weight corresponding to attachments in real coals is lumped into the two attachments in this modeling framework. Hence, the molecular weight of bridge material used in FLASHCHAIN is unrealistically high compared to chemical structure data (see, for example, Solum et al.¹⁵). Because of the use of unrealistic chemical structure parameters, vapor pressure coefficients are used as fitting parameters in the overall model in order to fit tar and total volatiles yields.

In the CPD model, the coal structure is approximated by a loopless tree structure called a Bethe lattice. The coordination number in the Bethe lattice has a minimum value of 2 in a fully connected lattice. The use of percolation statistics pertaining to a Bethe lattice permits an efficient closed-form solution for the relationship between the number of broken bridges and the mass of finite fragments. Niksa and Kerstein first used a Bethe lattice in a limited way,^{16,17} which provided some of the initial motivation for development of the CPD model.⁹ Solomon and co-workers recently incorporated a version of a Bethe lattice into a devolatilization model and discussed the relationship between several network models.¹⁸

The first version of the chemical percolation model⁹ demonstrated the ability of percolation lattice statistics, coupled with a coal pyrolysis mechanism, to describe a limited set of data reported by Serio and co-workers.⁸ In the CPD model, percolation lattice statistics are employed to describe the process of labile bridge scission to form lattice fragments of finite size. The initial CPD model was applied only to a narrow range of heating rates and temperatures. An extended version of this model explored the temperature dependence of the competition between the bridge scission rate (leading to tar formation) and the char bridge formation rate.¹⁹ All of the fragments of finite size were assumed to be released as tar in early versions of this model. Rate coefficients for the CPD model were obtained by comparison of model predictions with tar and total volatiles yield data from several coals of different rank over a wide range of temperature and heating rates at atmospheric pressure. The prediction of pressure-dependent devolatilization behavior was not possible, since the feature of the percolation statistics pertaining to the relative mass fraction and molecular weight of each fragment size was not fully treated in either of the two previous publications. The research discussed here exploits these features, permitting calculation of the molecular weight distribution of the finite fragments formed during bridge scission and the treatment of pressure effects. The addition of these features to the CPD model also permits direct use of chemical structure parameters of the parent coal, as measured by ^{13}C NMR spectroscopy, without sacrificing agreement with experimentally measured tar and total volatiles yields.

In this work, the chemical percolation model is extended to treat the distinction between low molecular weight aromatic fragments that vaporize as tar and high molecular

(11) Solomon, P. R.; Hamblen, D. G.; Carangelo, R. M.; Serio, M. A.; Deshpande, G. V. *Energy Fuels* 1988, 2, 405.

(12) Niksa, S.; Kerstein, A. R. *Combust. Flame* 1986, 66, 95.

(13) Niksa, S. *AIChE J.* 1988, 34, 790.

(14) Niksa, S.; Kerstein, A. R. *Energy Fuels* 1991, 5, 647.

(15) Solum, M. S.; Pugmire, R. J.; Grant, D. M. *Energy Fuels* 1989, 3, 187.

(16) Niksa, S.; Kerstein, A. R. *Fuel* 1987, 66, 1389.

(17) Kerstein, A. R.; Niksa, S. *Macromolecules* 1987, 20, 1811.

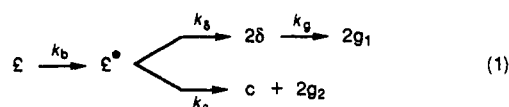
(18) Solomon, P. R.; Hamblen, D. G.; Yu, Z.; Serio, M. A. *Fuel* 1990, 69, 754.

(19) Fletcher, T. H.; Kerstein, A. R.; Pugmire, A. R.; Grant, D. M. *Energy Fuels* 1990, 4, 54.

weight fragments that remain with the char in a liquid or solid state as metaplast. The improved model includes a new vapor pressure correlation which was developed from data on coal liquids. The vapor pressure correlation compares well with tabulated vapor pressure data for a wide variety of pure organic components. The additions to the model allow predictions of tar molecular weights and yields as a function of residence time, temperature, and pressure. In contrast to previous efforts where model input parameters describing chemical structure are adjusted to force agreement between predicted and measured tar and total volatiles yields, coal-dependent chemical structure coefficients for the CPD model are taken directly from ^{13}C NMR analyses of parent coals. This procedure eliminates most adjustable parameters from the model, and predictions of tar and total volatiles yields become true tests of the model and the NMR data, rather than mere results of curve-fitting. Resulting model predictions of tar and total volatiles yields as a function of coal type, temperature, heating rate, and pressure compare well with available experimental data, showing the value of both the model and the NMR chemical structure data.

Theory

(a) Review of the CPD Model. Coal is treated in the CPD model as a macromolecular network of aromatic ring clusters of various sizes and types which are connected by a variety of chemical bridges of different bond strengths. For simplicity, only two types of bridges are treated: labile bridges and stable or char bridges. The reaction sequence is represented as follows:



A labile bridge, represented by \mathcal{L} , decomposes to form a reactive bridge intermediate, \mathcal{L}^* , which is unstable and reacts quickly in one of two competitive reactions. In one reaction pathway, the reactive intermediate bridge, \mathcal{L}^* , is cleaved, and the two halves form side chains, δ , that remain attached to the aromatic cluster. Finite tar fragments are generated as a sufficient number of bridges are cleaved to form finite clusters that are completely detached from the infinite lattice network. The side chains, δ , eventually undergo a cracking reaction to form light gas g_1 . In a second, competing reaction pathway, the reactive intermediate, \mathcal{L}^* , is stabilized to form a stable "char" bridge, c , with the associated release of light gas, g_2 . In this work, all mass connected to the infinite lattice is referred to as char and is normalized by the initial amount of coal. Finite fragments that remain in the condensed phase are referred to as metaplast. At any instant, then, the initial coal mass is divided into light gas, tar, metaplast, and char. From a chemical viewpoint, a portion of the material defined in this context as char includes any unreacted coal, as reflected in the fact that infinite lattices consist of labile bridges as well as stabilized char bridges during pyrolysis. The percolation statistics determine the populations of finite fragments (i.e., tar plus metaplast) as a function of the ratio of intact to broken bridges. A vapor-liquid equilibrium scheme (described later) determines the fraction of finite fragments that are vaporized as tar.

The competition for the reactive intermediate \mathcal{L}^* is governed by the ratio of the rate of side-chain formation to the rate of char formation. The dynamic variables of the theory are the bridge population parameters, \mathcal{L} and c , and the side chain parameter δ . The associated kinetic expressions for the proposed reaction mechanism (eq 1)

are presented and discussed by Grant et al.⁹ and the reader is directed to that work for the mathematical details.

In the CPD model, bridge population parameters are normalized by the total number of bridges possible in the fully connected lattice. The terminology used in this paper is changed slightly from that used by Grant et al.⁹ in order to compare model results with additional NMR data. The terms "sites" and "clusters" used by Grant et al.⁹ are referred to in this work as "clusters" and "fragments", respectively. Finite fragments formed from bridge scission may consist of one aromatic cluster (monomer), two clusters connected by a labile or char bridge (dimer), or n clusters (fragment size n) connected by $n - 1$ bridges. As indicated by eq 36 of Grant et al.,⁹ the mass of a finite fragment of size n , generated as a function of time by labile bridge scission, is calculated from the bridge population parameters \mathcal{L} and p as follows:

$$m_{\text{frag},n} = nm_a + (n - 1)m_b(\mathcal{L}/p) + \tau m_b(\delta/4)(1 - p) \quad (2)$$

The first term in eq 2 represents the molecular weight of the n clusters in a fragment ($n = 1$ is a monomer, such as benzene, toluene or naphthalene; $n = 2$ is a dimer, such as two benzenes connected by an aliphatic bridge; etc.). The second term is the molecular weight of labile bridges m_b multiplied by the fraction of intact labile bridges $(n - 1)\mathcal{L}/p$. Finally, the third term provides the molecular weight of side chains to be released as gas, and is calculated from the fraction of side chains, $\delta/2(1 - p)$, times the number of broken bridges τ , times the mass of each side chain $m_\delta = m_b/2$. The total mass associated with fragments of size n is the mass of the fragment $m_{\text{frag},n}$ multiplied by the population of those fragments, as follows:

$$m_{\text{fin},n} = m_{\text{frag},n} Q_n(p) = \left\{ nm_a + (n - 1)m_b(\mathcal{L}/p) + \frac{\tau m_b \delta}{4(1 - p)} \right\} Q_n(p) \quad (3)$$

In this equation, $Q_n(p) = F_n(p)/n$ is the population of n -cluster fragments, expressed on a per cluster basis.⁹ The total mass associated with the finite fragments (assumed to be the tar mass in previous formulations of the CPD model^{9,19}) is obtained by summing the contributions from each fragment size, as follows:

$$m_{\text{fin}}(t) = \sum_{n=1}^{\infty} m_{\text{fin},n}(t) \quad (4)$$

The material extracted from parent coals using suitable solvents (such as tetrahydrofuran) corresponds to the bitumen, or finite fragments trapped in the coal at room temperature and pressure. This material is the first to vaporize from the coal as it is heated, since no bonds are broken to form the finite fragments prior to vaporization.²⁰ Many highly polar solvents such as pyridine extract colloidal dispersions along with the bitumen, which are agglomerates of material with extremely large molecular weights ($\sim 10^6$ amu), and hence extract yields using such solvents are not representative of material that would vaporize during heating. Hence, in the CPD model, unlike in other models,^{11-14,18} pyridine extract yield data are not used as input parameters. The initial mass fraction of finite fragments in the parent coal is calculated in the CPD model from the bridge population parameters \mathcal{L}_0 , c_0 , and $f_{\text{gas},\infty}$ using percolation statistics.

The finite fragments formed as a result of bridge scission may undergo a phase change to form a vapor, dependent

(20) Chakravarty, T.; Windig, W.; Hill, G. R.; Meuzelaar, H. L. C.; Khan, M. R. *Energy Fuels* 1988, 2, 400.

upon the pressure, temperature, and molecular weight. At a given temperature and pressure, the low molecular weight species (e.g., benzene, naphthalene) exhibit high vapor pressures, causing significant quantities to be released as vapor. As pyrolysis products are cooled to room temperature and pressure, however, many of these species condense to form liquids and solids and hence are classified as tar. Species that do not condense at room temperature and pressure are considered light gas and are treated separately.⁹ High molecular weight species with low vapor pressures that do not vaporize at reaction temperatures and pressures remain in a liquid or solid state in the char matrix. Hence, a fragment of intermediate molecular weight may be metaplast at one temperature and tar vapor at an elevated temperature. The nonvaporized material that is detached from the infinite coal matrix is termed metaplast.

In the present work, the effect of vapor pressures on gas-phase pyrolysis products is modeled assuming a simple form of Raoult's law, requiring the development of an empirical expression describing the vapor pressures of high molecular weight organic molecules (in the range 200–1000 amu). Previous generalized vapor pressure expressions were developed for only a limited set of species at very low pressures. The Raoult's law expression and the vapor pressure correlation are combined with a standard flash distillation calculation at each time step to determine the partitioning between vapor and liquid for each finite fragment size, in a manner similar to that used by Niksa^{13,14} and by Solomon and co-workers.¹¹ Equilibrium between escaped tar and trapped metaplast is used to demonstrate the capability of the improved CPD model to describe pressure-dependent tar yields and molecular weight distributions. The Raoult's law formulation, development of the generalized vapor pressure expression, and the flash distillation equations are described below.

(b) Raoult's Law. In a treatment similar to the flash vaporization scheme proposed by Niksa,¹³ it is assumed that the finite fragments undergo vapor/liquid phase equilibration on a time scale that is rapid with respect to the chemical bond scission reactions. As an estimate of the amount of vapor and liquid present at any time, Raoult's law is invoked; the partial pressure P_i of a substance is proportional to the vapor pressure of the pure substance P_i^v multiplied by the mole fraction of the substance in the liquid x_i :

$$P_i = y_i P = x_i P_i^v \quad (5)$$

where y_i is the mole fraction of the species in the vapor phase. This simple form of Raoult's law assumes ideal activity coefficients, since this type of data is not generally available for large molecular weight organic species. The total pressure P is the sum of the partial pressures of the different gaseous species:

$$P = \sum_{i=1}^{\infty} y_i P = \sum_{i=1}^{\infty} P_i \quad (6)$$

(c) Vapor Pressures of High Molecular Weight Organic Molecules. Vapor pressure data for coal tar are unavailable, so vapor pressure correlations based on compounds found in coal tar are generally used. Unger and Suuberg²¹ proposed a vapor pressure correlation based on boiling points of six aromatic hydrocarbons²² at a total pressure of 6.6×10^{-4} atm (0.5 mmHg). These compounds

were selected because of their high molecular weight (198–342) and their lack of heteroatoms. The resulting correlation developed by Unger and Suuberg is

$$P_i^v = \alpha \exp(-\beta M_i^\gamma / T) \quad (7)$$

where $\alpha = 5756$, $\beta = 255$, and $\gamma = 0.586$, and units are in atmospheres and kelvin. The form of eq 7 can be obtained from the Clausius–Clapeyron equation, assuming that the heat of vaporization is proportional to molecular weight. Equation 7 is the simplest thermodynamic expression relating vapor pressure, temperature, and molecular weight²³ and is used because of the lack of detailed chemical structure and vapor pressure data on coal tar.

Several investigators have attempted to use the Unger–Suuberg correlation to describe tar release from metaplast. Many investigators use the form of the Unger–Suuberg correlation, but not the constants proposed by Unger and Suuberg. Solomon and co-workers¹¹ used the Unger–Suuberg correlation multiplied by a factor of 10 in order to fit tar and total coal volatiles yields as a function of pressure, although recently the factor of 10 was eliminated by changing other input parameters.²⁴ Niksa¹³ used a similar form that was easy to integrate analytically, with $\gamma = 1$, and α and β as adjustable parameters to fit tar molecular weight data from Unger and Suuberg.²⁵ All three vapor pressure coefficients are treated as adjustable parameters in recent work by Niksa.^{13,14} Oh and co-workers²⁶ and Hsu²⁷ found that by using the Unger–Suuberg correlation, good agreement could be achieved with high-temperature pyrolysis data ($T > 873$ K) but not with low-temperature data ($T < 873$ K). The current work suggests why the Unger–Suuberg correlation is limited at typical coal pyrolysis conditions and gives a similar but alternate correlation.

The vapor pressure correlation of Unger and Suuberg²¹ is based on data at low vapor pressures (0.5 mmHg) but has been extrapolated to much higher pressures and molecular weights in coal devolatilization models. Reid et al.²³ recommended using the Antoine equation to calculate vapor pressures (if constants are available) when the vapor pressure is in the range 10–1500 mmHg (0.01–2 atm). However, Reid and co-workers conclude that no correlation produces good agreement with data for $P_i^v < 10$ mmHg (0.01 atm). The approach used here is to develop new constants for eq 7 based on additional data at both low and high vapor pressures in order to treat a wide range of coal pyrolysis conditions. The use of the resulting vapor pressure correlation eliminates some of the uncertainties in developing input parameters for coal pyrolysis models.

Gray et al.^{28,29} measured vapor pressures as a function of temperature for 12 narrow boiling point fractions distilled from coal liquids produced from SRC-II processing of Pittsburgh seam bituminous coal. In their study, temperatures ranged from 267 to 788 K, the coal liquids exhibited molecular weights ranging from 110 to 315 amu, and the lightest fractions exhibited vapor pressures as high as 35 atm. It is assumed that these are representative of

(23) Reid, R. C.; Prausnitz, J. M.; Sherwood, T. K. *Properties of Gases and Liquids*, 3rd ed.; McGraw-Hill: San Francisco, 1977; p 196.

(24) Solomon, P. R.; Hamblen, D. G.; Serio, M. A.; Yu, Z.; Charpenay, S. *ACS Div. Fuel Chem. Prepr.* 1991, 36, 267.

(25) Unger, P. E.; Suuberg, E. M. *Fuel* 1984, 63, 606.

(26) Oh, M. S.; Peters, W. A.; Howard, J. B. *AIChE J.* 1989, 35, 775.

(27) Hsu, J. Sc.D. Thesis, Department of Chemical Engineering, Massachusetts Institute of Technology, 1989.

(28) Gray, J. A.; Brady, C. J.; Cunningham, J. R.; Freedman, J. R.; Wilson, G. M. *Ind. Eng. Chem. Process Des. Dev.* 1983, 22, 410.

(29) Gray, J. A.; Holder, G. D.; Brady, C. J.; Cunningham, J. R.; Freedman, J. R.; Wilson, G. M. *Ind. Eng. Chem. Process Des. Dev.* 1985, 24, 97.

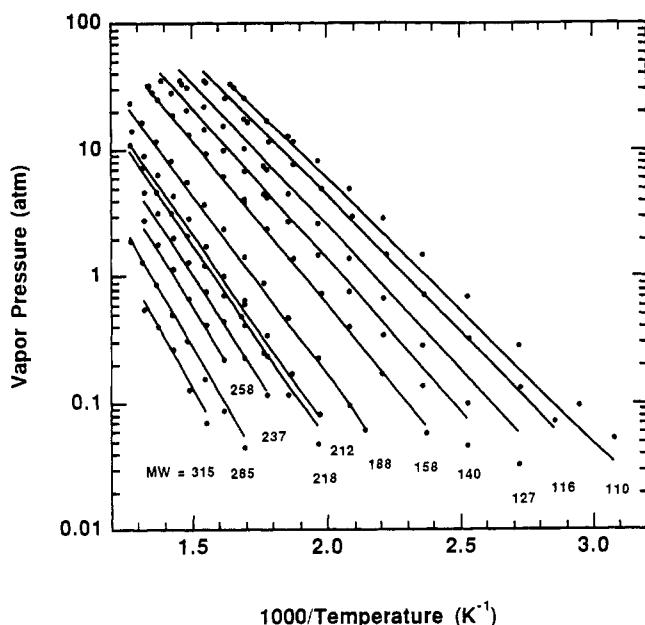
(21) Unger, P. E.; Suuberg, E. M. *ACS Div. Fuel Chem. Prepr.* 1983, 28, 278.

(22) Smith, G.; Winnick, J.; Abrams, D. S.; Prausnitz, J. M. *Can. J. Chem. Eng.* 1974, 54, 337.

Table I. Vapor Pressure Correlations for Coal Pyrolysis Tar and Metaplast

$$P_i = \alpha \exp(-\beta MW_i^\gamma / T)$$

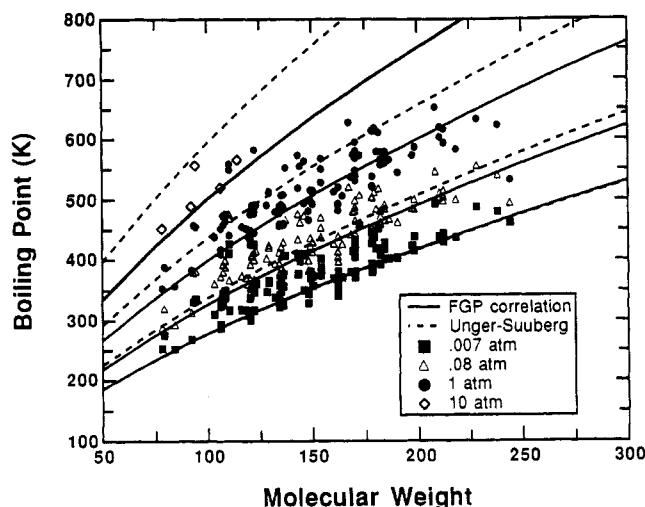
	α	β	γ
Unger-Suuberg ²¹	5756	255	0.586
Niksa ¹³	70.1	1.6	1.0
Niksa and Kerstein ¹⁴	3.0×10^5	200	0.6
FGP (this work)	87060	299	0.590

**Figure 2.** Comparison of the Fletcher-Grant-Pugmire vapor pressure correlation with vapor pressure data from Gray, et al.^{28,29} for 12 narrow boiling point fractions of coal liquids from a Pittsburgh seam coal.

low molecular weight tars released during primary pyrolysis. Gray and co-workers discuss equations of state that fit the vapor pressure data using critical properties of the liquid (i.e., the critical temperature and pressure). However, for the purposes of coal pyrolysis, critical properties are not well-known, and simpler correlations are needed.

A new correlation was generated by curve-fitting the data of Gray et al.^{28,29} using eq 7; the new coefficients are shown in Table I. This correlation, referred to as the Fletcher-Grant-Pugmire (FGP) correlation, agrees well with the measured vapor pressures of the different molecular weight fractions, as shown in Figure 2. Coefficients for the vapor pressure expressions used by other investigators are also shown in Table I. It is interesting that the coefficient on the molecular weight (γ) from the curve-fit to the data of Gray and co-workers is 0.590, which is very close to the value of 0.586 found by Unger and Suuberg. The value of β from the Unger-Suuberg correlation is 255, which compares reasonably well with the value of 299 in the FGP correlation. The major difference between the two correlations is the value for α ; the value of α in the FGP correlation is 15 times greater than in the Unger-Suuberg correlation. This is somewhat consistent with modeling efforts¹¹ where the vapor pressure from Unger-Suuberg correlation was multiplied by a factor of 10 in order to achieve agreement with a wide range of experimental data.

The FGP vapor pressure correlation was also compared with boiling point data at pressures of 5, 60, 760, and 7600 mmHg (0.0066, 0.079, 1.0, and 10 atm) for a set of 111 pure organic compounds that are thought to be present in coal-derived liquids. Boiling point data are from Perry and

**Figure 3.** Comparison of the Fletcher-Grant-Pugmire (FGP) vapor pressure correlation and the Unger-Suuberg vapor correlation with boiling point data for 111 organic compounds at pressures of 0.007, 0.08, 1, and 10 atm (5, 60, 760, and 7600 mmHg).

Chilton;³⁰ a list of the selected compounds is available.³¹ Molecular weights as high as 244 are considered in this set of compounds. Long-chain alkanes (hydrogen to carbon ratios greater than 1.5) and heteroatoms with more than two oxygen atoms are not considered in this data set, since they do not occur in coal tars to a significant extent. Boiling point data at 10 atm are available only for five compounds.³¹ The FGP correlation was found to agree surprisingly well with the boiling points of these compounds at all four pressures, as shown in Figure 3. This is a simplistic vapor pressure expression; other vapor pressure expressions that take into account the variations in the chemical structures of the various compounds²³ are not considered. The correlation proposed by Unger and Suuberg²¹ agrees with this set of data at the lowest pressure but predicts higher boiling points than the data at pressures of 1 and 10 atm (see Figure 3).

The six data points used to develop the Unger-Suuberg correlation²¹ were taken from Smith et al.;²² the FGP correlation also agrees well with these same six data points. The sum-square error of the FGP correlation with regard to these six boiling points is actually 12% less than that obtained using the Unger-Suuberg correlation. The similarity of the two correlations at low vapor pressures suggests the need for careful examination of the two correlations versus data at a wide range of temperatures and pressures. The Unger-Suuberg correlation was found to yield poor agreement with the data of Gray et al.;^{28,29} predicted vapor pressures were 3 times lower than the data at 35 atm.

Coal pyrolysis experiments have been conducted at pressures as high as 69 atm,³² with reported tar molecular weight distributions extending into several thousand amu. Figure 4 shows an extrapolation of three vapor correlations to higher temperatures, pressures, and molecular weights than shown in Figure 3, representing a wide range of pyrolysis conditions. The difference between the FGP correlation and the Unger-Suuberg correlation becomes more

(30) Perry, R. H.; Chilton, C. H. *Chemical Engineers' Handbook*, 5th ed.; McGraw-Hill: San Francisco, 1973; pp 3-49.

(31) Fletcher, T. H.; Hardesty, D. R. *Coal Combustion Science: Task 1, Coal Devolatilization*. DOE/PETC Quarterly Progress Report for January to March, 1990, Hardesty, D. R., ed.; Sandia Report No. SAND90-8223, available NTIS.

(32) Suuberg, E. M.; Peters, W. A.; Howard, J. B. *Seventeenth Symp. (Int.) Comb.*; The Combustion Institute: Pittsburgh, PA, 1978; p 117.

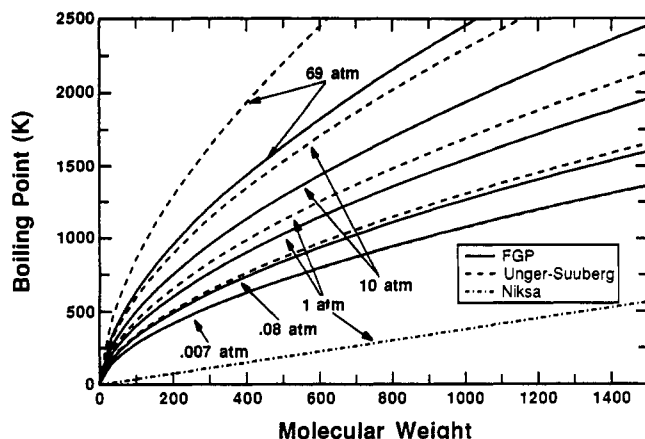


Figure 4. Comparison of the FGP (this work), Unger-Suuberg,²¹ and Niksa¹³ vapor correlations for molecular weights as high as 1500 and pressures as high as 69 atm.

pronounced at higher pressures. For example, the predicted boiling point of a species with a molecular weight of 400 amu by the FGP correlation is nearly 500 K lower than that predicted by the Unger-Suuberg correlation. In contrast, the parameters in the vapor pressure correlation used by Niksa^{13,14} were used as fitting parameters to achieve agreement with measured molecular weight distributions. In FLASHCHAIN, two sets of vapor pressure coefficients are presented; one set for predictions with recombination kinetics, and one set when recombination kinetics are neglected. The boiling points predicted by the correlation used by Niksa and Kerstein¹⁴ at a pressure of 1 atm follows the 0.007 atm curve from the FGP correlation in Figure 4 and are not shown. For a molecular weight of 400 amu, the two Niksa correlations give boiling points at atmospheric pressure that are respectively 800 and 300 K lower than predicted by the FGP correlation, illustrating that unrealistic solutions can be obtained when vapor pressure coefficients are used as adjustable parameters. The FGP vapor correlation agrees with measured vapor pressures of coal liquids and boiling points of pure compounds over a wide range of pressures. The coefficients α , β , and γ used in the correlation are fixed by independent data, thereby reducing the number of unknown parameters in coal pyrolysis models.

(d) Flash Distillation. The mass of finite fragments can be used as the feed stream of a flash distillation process, where vapor-liquid equilibrium is achieved. The approach to flash distillation is patterned after the method outlined by King.³³ If f_i = the moles of species i before vapor-liquid equilibrium, l_i = the moles of species i in the metaplast after vapor-liquid equilibrium, and v_i = the moles of species i in the vapor phase after vapor-liquid equilibrium, then the following relations apply:

$$f_i = v_i + l_i \quad (8)$$

$$F = V + L \quad (9)$$

where

$$F = \sum f_i \quad V = \sum v_i \quad L = \sum l_i \quad (10)$$

$$f_i = z_i F \quad v_i = y_i V \quad l_i = x_i L \quad (11)$$

Vapor-liquid relationships are expressed in the form

$$y_i = K_i x_i \quad (12)$$

Substituting this expression for y_i into eq 8 yields

$$z_i F = K_i x_i V + x_i L = x_i (F - V) + x_i K_i V \quad (13)$$

This equation is rearranged to provide an expression for x_i :

$$x_i = \frac{z_i}{(K_i - 1)(V/F) + 1} \quad (14)$$

Following recommendations by Rachford and Rice,³⁴ the identity

$$\sum y_i - \sum x_i \equiv 0 \quad (15)$$

can be used with eqs 12 and 14 to provide a stable equation for iterative numerical solution:

$$f\left(\frac{V}{F}\right) = \sum_i \frac{z_i (K_i - 1)}{(K_i - 1)(V/F) + 1} = 0 \quad (16)$$

This equation is in a form with relatively linear convergence properties, with no spurious or imaginary roots.³³ Other forms of solution present highly nonlinear functions, which often lead to imaginary roots. The secant method (e.g., Gerald³⁵) is used to solve for V/F from eq 16, and eqs 12 and 14 are used to obtain x_i and y_i .

(e) Mass Transfer Considerations. The application of the flash distillation equations to coal tar evolution requires appropriate assumptions regarding the location and amount of material that is in vapor-liquid equilibrium. Different theoretical treatments of mass-transfer effects on coal tar evolution are reviewed by Suuberg.⁷ For example, Oh, et al.²⁶ and Hsu²⁷ used bubble transport models to describe intraparticle transport of tar and gases. In simpler approaches used by Solomon et al.¹¹ and by Niksa,^{13,14} the tar vapor is convected from the particle by the light gas, and it is assumed that the volume of vaporized tar is small compared to the volume of evolved light gas. Other approaches allow for the possibility that some liquid from the metaplast may be entrained in the light gas in an attempt to explain reported molecular weights greater than 1000 amu,⁷ where the molecular weights is too high to allow vaporization.

In the CPD model, the assumption is made that all gaseous species (light gases and tar vapors) are convected away from the particle due to the increase in volume between the gas and solid. This approach is similar to that used by Solomon et al.¹¹ and by Niksa.^{13,14} The convection step is assumed to be rapid compared with the chemical reactions of bond scission and char formation. Convection of liquid metaplast by gases and tar vapors is thought to be of secondary importance, based on recent measurements of tar molecular weights,^{11,36} and is ignored in this work. This is consistent with experimental results of Suuberg et al.,³⁷ which indicate that tar evaporation is more important than transport of liquid tar by light gas. The vapor pressures predicted by the FGP correlation drop steeply with molecular weight, implying that there is little vaporization of high molecular weight compounds. In other words, most of the tar vapor at a given temperature consists of compounds with vapor pressures higher than the ambient pressure. It is assumed that the volume of tar vapor alone is sufficient to cause rapid evolution from the vicinity of the particle, without the necessity of transport by lighter gases. The presence of light gas is not necessary

(34) Rachford, H. H., Jr.; Rice, J. D. *Pet. Technol.* 1952, 4, section 1, p 19; section 2, p 3.

(35) Gerald, C. F. *Applied Numerical Analysis*; Addison Wesley: Menlo Park, CA, 1978; p 11.

(36) Freihaut, J. D.; Proscia, W. M.; Seery, D. J. *Energy Fuels* 1989, 3, 692.

(37) Suuberg, E. M.; Unger, P. E.; Lilly, W. D. *Fuel* 1985, 64, 956.

(33) King, C. J. *Separation Processes*; McGraw-Hill: San Francisco, 1970; pp 70-71, 511-512.

for tar release by a convective flow mechanism, since the phase change from liquid metaplast to tar vapor increases the volume by 2–3 orders of magnitude.

Only the tar and light gas formed in the last time step are considered to be in vapor–liquid equilibrium with the metaplast. This is analogous to a plug flow reactor, in that the tar and light gas formed at earlier residence times does not mix with newly formed pyrolysis products. The amount and molecular weight distribution of the tar and light gas formed at each time step is stored for use in the flash distillation calculation for the next time step. The computed results are therefore time-step dependent unless care is taken to use small time increments during periods of rapid tar release. To maintain computational efficiency, a numerical scheme was implemented that adjusts the time step based on the rate of reaction.

(f) Cross-Linking. Large amounts of high molecular weight compounds are generated during the pyrolysis of bituminous coals, as evidenced by solvent extraction experiments. Fong and co-workers³⁸ measured the amount of pyridine extracts from coal chars as a function of residence time at moderate heating conditions (~500 K/s). A maximum of 80% of the original coal was either released as volatile matter or extracted with pyridine during these experiments. However, at the completion of volatiles release, very small amounts of pyridine extractables were obtained. The final volatiles yield was approximately 40% in these experiments; the additional amount of pyridine extractables (approximately 40%) was in some manner cross-linked to the char matrix before the end of devolatilization. The pyridine extract data are viewed as a qualitative description of the amount of metaplast existing in the coal. However, pyridine extracts contain significant quantities of colloidal dispersed material (molecular weights of 10⁶ amu or higher), and hence these data should not be used quantitatively.

Additional experiments have been performed to characterize the extent of cross-linking in coal chars during devolatilization. Solvent swelling measurements of coal chars are interpreted as indications of the extent of cross-linking.^{39,40} Solid-state ¹³C NMR measurements of the chemical structure of coal chars also show an increase in the number of bridges and loops between aromatic clusters in the final stages of mass release,^{41,42} indicative of cross-linking. The importance of cross-linking was illustrated in a recent comparison of an earlier formulation of the CPD model that did not treat cross-linking (or vapor–liquid equilibrium) with models that include treatments of cross-linking.¹⁸

A simple cross-linking mechanism is used in this work to account for the reattachment of metaplast to the infinite char matrix. The rate of cross-linking is described using a simple, one-step Arrhenius rate expression:

$$dm_{\text{cross}}/dt = -dm_{\text{meta}}/dt = k_{\text{cross}}m_{\text{meta}} \quad (17)$$

where m_{meta} is the mass of metaplast, m_{cross} is the amount of metaplast that has been reattached to the infinite char matrix, and k_{cross} is the Arrhenius rate constant [$k_{\text{cross}} = A_{\text{cross}} \exp(-E_{\text{cross}}/RT)$].

The mass of metaplast is updated at each time step, based on (1) the amount of finite fragment material gen-

erated during labile bridge scission, according to the percolation statistics and (2) the flash distillation submodel and vapor pressure relationship. The amount of metaplast that has been reattached to the infinite char matrix during each time step is calculated and added to the mass of the char. For simplicity, the metaplast that is reattached to the char is assumed to uniformly decrease the concentration of all fragment size bins on a mass basis. In other words, one rate of reattachment (on a mass basis) is used, independent of fragment size. In reality, the fragments containing many clusters contain the most sites for reattachment⁹ and should therefore cross-link faster (on a number basis) than compounds with one or two clusters. However, since the concentration of each fragment size decreases monotonically with the number of clusters, very few fragments with large numbers of clusters exist. At the present time, there is no mechanistic or empirical basis for the use of separate cross-linking rates for each fragment size bin, and errors introduced by assuming uniform cross-linking rates are thought to be small.

The cross-linking mechanism in the CPD model is decoupled from the percolation statistics. For bituminous coals, the crosslinking occurs subsequent to tar release,^{41,42} meaning that the labile bridge scission and the reattachment of finite clusters occur in series. For low-rank coals, such as lignites, there is evidence for cross-linking before significant tar release.^{39,40,42,43} This type of early cross-linking is treated in the selection of initial chemical structure parameters for the CPD model and will be formally treated in a subsequent investigation.

It is assumed that the cross-linking process does not introduce an additional mechanism for light gas release, so that the population of side chains is not affected by the cross-linking reaction. However, tar that is released from the particle may contain labile bridges (\mathcal{L}), char bridges (c), and side chains (δ). The initial description of the CPD model allowed for reactions of tar in the gas phase after release from the particle.^{9,19} In this work, secondary tar reactions in the gas phase are not treated in order to permit comparison with devolatilization experiments such as heated grids where the tar is quenched after leaving the vicinity of the particle. The side chains released with the tar must therefore be subtracted from the pool of side chains available to form light gas from the char and metaplast. The number of side chains, δ , is calculated from the percolation statistics, which are decoupled from the flash distillation and cross-linking mechanisms, as described by Grant et al.:⁹

$$\frac{d\delta}{dt} = \frac{2\rho k_b \mathcal{L}}{\rho + 1} - k_g \delta \quad (18)$$

where k_g is the rate constant for light gas formation from side chains (g_1). Variables used here are the same as defined by Grant et al.,⁹ a complete nomenclature is provided at the end of this paper. The first term on the right-hand side of eq 18 represents the formation of side chains due to labile bridge scission, and the second term represents the release of side chains as light gas, g_1 . The mass of light gas formed from side chains is calculated from an algebraic relationship:

$$g_1 = 2(1 - p) - \delta \quad (19)$$

where p is the number of intact bridges ($\mathcal{L} + c$). The first term in eq 19 represents the total number of broken labile

(38) Fong, W. S.; Peters, W. A.; Howard, J. A. *Fuel* 1986, 65, 251.

(39) Suuberg, E. M.; Lee, D.; Larsen, J. W. *Fuel* 1985, 64, 1668.

(40) Solomon, M. A.; Serio, M. A.; Deshpande, G. V.; Kroo, E. *Energy Fuels* 1990, 4, 42.

(41) Fletcher, T. H.; Solum, M. S.; Grant, D. M.; Critchfield, S.; Pugmire, R. J. *Twenty-Third Symp. (Int.) Comb.* 1990, 1231.

(42) Pugmire, R. J.; Solum, M. S.; Grant, D. M.; Critchfield, S.; Fletcher, T. H. *Fuel* 1991, 70, 414.

(43) Fletcher, T. H.; Hardesty, D. R. *Coal Combustion Science: Task 1, Coal Devolatilization*. DOE/PETC Quarterly Progress Report for June to September, 1990; Hardesty, D. R., Ed.; Sandia Report No. SAND90-8247, available NTIS.

bridges (which are split into two pieces), and the second term represents the number of side chains remaining. Additional light gas, g_2 , is released during the stabilization of labile bridges to form char bridges. The amount of light gas formed during char formation is calculated from the change in the char bridge population:

$$g_2 = 2(c - c_0) \quad (20)$$

In the initial description of the CPD model,^{9,19} the labile bridges and side chains in the evolved tar continued to react at the same temperature as the particle; a gradual decrease in tar yield was accompanied by a corresponding increase in gas yield at long residence times. In a combustion environment, this stimulates the thermal cracking of tar and the initial stages of soot formation. However, in the present formulation, gas phase reaction of tar is not calculated, and only the amount of gas released from the char and metaplast is treated. To account for the decrease of gas precursors as tar is released, the mass of gas formed (m'_{gas}) is normalized by the tar yield as follows:

$$m'_{gas} = m_{gas}(1 - f_{tar}) \quad (21)$$

where f_{tar} is the mass fraction of coal evolved as tar and m'_{gas} is the normalized amount of gas. This is an approximate normalization procedure, and assumes that the concentrations of labile bridges, char bridges, and side chains in the tar are equal to the respective concentrations in the combination of metaplast, cross-linked metaplast, and the infinite char lattice. This assumption is good to first order, but small errors are introduced because the tar consists of only the light molecular weight fragments (monomers and dimers) and hence should contain a slightly different concentration of side chains than the metaplast and infinite char lattice. The alternative to this assumption is an extensive accounting procedure of molecular fragment bins with appropriate exchange coefficients, as used by Niksa and Kerstein.¹⁴ Errors introduced by this assumption are small, and the CPD model does not include this complexity for the present.

Selection of Model Input Parameters

The relation of model input parameters to actual chemical and physical properties of the coal, developed below, establishes the mechanistic basis of the model and facilitates extrapolation to other coal types and operating conditions.

(a) Rate Parameters. Use of the CPD model requires specification of three rates: the rate of labile bridge scission, the rate of light gas release, and the rate of cross-linking. These kinetic rates are assumed to be coal-independent; only the chemical structure determines differences in devolatilization behavior due to coal type. In addition, the composite rate coefficient ρ relating the rate of side chain formation to the rate of char bridge formation must also be specified. A discussion of the rate parameters for the bridge scission, gas release, and char formation reactions is provided in earlier publications.^{9,19} The value of E_b in the CPD model was set at 55 kcal/mol, as reported by Serio and co-workers.⁸ The devolatilization rates reported by Serio, obtained using temperature measurements of particle clouds, agree with rates measured by Fletcher,^{44,45} where individual particle temperatures were measured during devolatilization. A weighted average of the activation energies for light gas release reported by Serio resulted in $E_g = 69$ kcal/mol. The data of Serio were curve-fit using the CPD model to obtain values for A_b , V_b ,

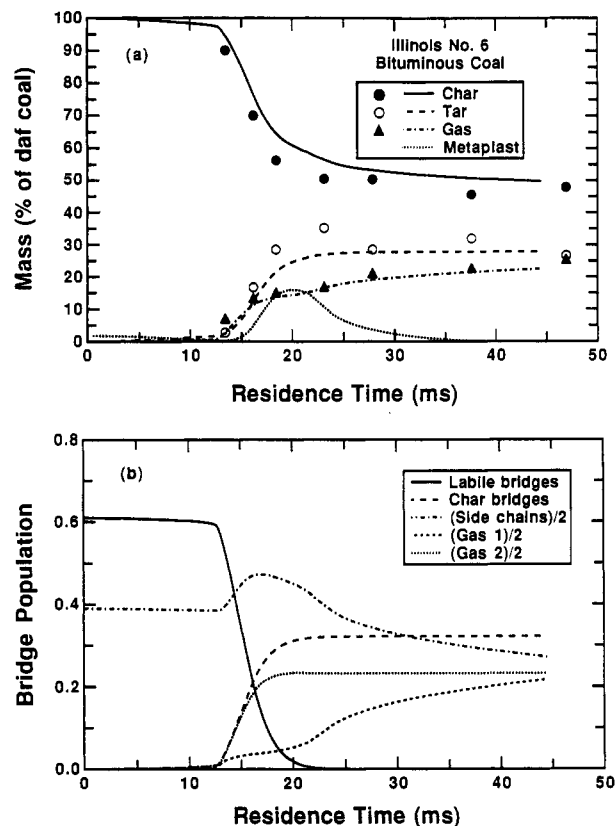


Figure 5. (a) CPD calculations of devolatilization yields of char, tar, and light gases versus time for Illinois No. 6 high volatile bituminous coal. Experimental data are from Serio et al.⁸ and chemical structure parameters for the model are taken directly from NMR data (no adjustable parameters); (b) Bridge dynamic population parameters on a per site basis as a function of time (δ , g_1 , and g_2 variables are divided by two).

Table II. Rate Parameters Used in the CPD Model

parameter	value	description
E_b	55.4 kcal/mol	bridge scission activation energy
A_b	$2.6 \times 10^{15} \text{ s}^{-1}$	bridge scission frequency factor
σ_b	1.8 kcal/mol	standard deviation for distributed E_b
E_g	69 kcal/mol	gas release activation energy
A_g	$3 \times 10^{15} \text{ s}^{-1}$	gas release frequency factor
σ_g	8.1 kcal/mol	standard deviation for distributed E_g
ρ	0.9	composite rate constant k_b/k_c

A_g , and V_g . Results of this evaluation are shown in Figures 5–7, with resulting kinetic parameters given in Table II. As shown by Fletcher et al.,¹⁹ these kinetic parameters allow good agreement between predicted and measured coal devolatilization rates for heating rates ranging from 1 to 10^4 K/s. For example, a comparison of CPD model predictions with the data of Fletcher,^{43,44} which include measurements of single particle temperatures, is shown in Figure 8 for Illinois No. 6 coal particles (106–125- μm size fraction). As discussed below, chemical structure parameters for these model predictions were taken directly from NMR data, which was not possible with earlier model formulations that did not treat vapor–liquid equilibrium and cross-linking.

(b) Cross-Linking Rates. The use of the cross-linking mechanism in the CPD model requires specification of two additional rate parameters: E_{cross} and A_{cross} . Solomon and co-workers¹¹ used solvent swelling data to generate an empirical correlation between the rate of CH_4 release and the rate of cross-linking in high-rank coals ($E_{\text{CH}_4} = 60$ kcal/mol). Other investigators have taken cross-linking rates from time-dependent pyridine extractables from coal chars during devolatilization (Fong et al.;³⁸ $E_{cross} = 42$

(44) Fletcher, T. H. *Combust. Sci. Technol.* 1989, 63, 89.

(45) Fletcher, T. H. *Combust. Flame* 1989, 78, 223.

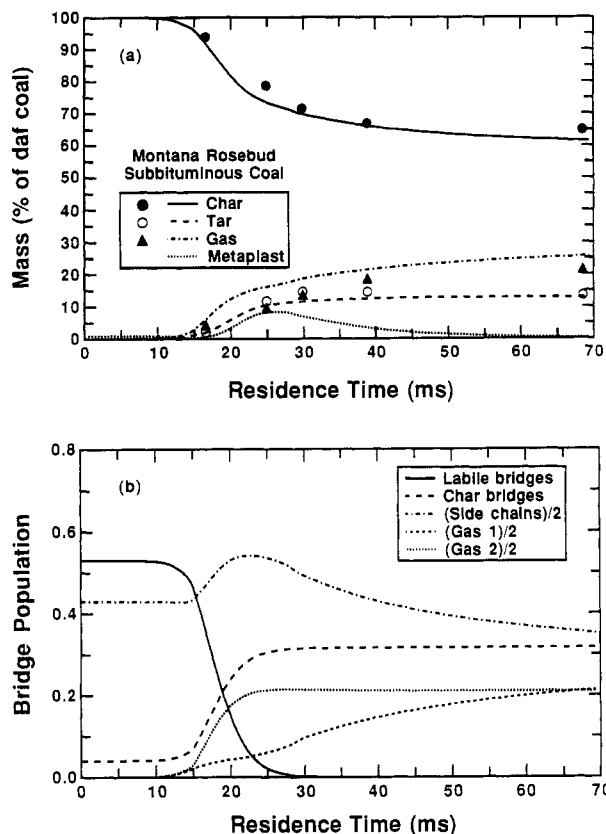


Figure 6. (a) CPD calculations of devolatilization yields of char, tar, and light gases versus time for Montana Rosebud subbituminous coal. Experimental data are from Serio et al.,⁸ and chemical structure parameters for the model are taken directly from NMR data (one adjustable parameter: c_0); (b) Bridge dynamic population parameters on a per site basis as a function of time (δ , g_1 , and g_2 variables are divided by 2).

kcal/mol). This section describes the rationale for the selection of the values of E_{cross} and A_{cross} used in the CPD model, and illustrates the sensitivity of the model to these parameters.

The cross-linking in bituminous coals occurs subsequent to tar release, as evidenced by the NMR data regarding the number of bridges and loops per aromatic cluster as a function of mass release.⁴¹ Therefore, the activation energy used for the cross-linking rate in the CPD model must be higher than that used for labile bridge scission (55 kcal/mol). A series of calculations was performed to determine the performance of the CPD model with three different values of E_{cross} (60, 65, and 70 kcal/mol). The preexponential factor A_{cross} was set to that used for gas release in the CPD model ($3.0 \times 10^{15} \text{ s}^{-1}$); this high value ensures rapid cross-linking after a threshold temperature is achieved. Model predictions using the three values of E_{cross} were compared with (a) temperature-dependent total volatiles yield data at different heating rates;⁴⁶ (b) time-dependent, pyridine extract yield data;³⁸ (c) NMR data regarding the number of bridges and loops per aromatic cluster.⁴¹ Results and interpretations are as follows:

Volatiles Yield Data. Gibbins-Matham and Kandiyoti⁴⁶ measured total volatiles yields from the Argonne premium Pittsburgh No. 8 coal as a function of temperature for three conditions: (i) 1000 K/s with a 30-s hold time at the final temperature; (ii) 1000 K/s with a 0-s hold time (immediate quench); (iii) 1 K/s with immediate quench. At temperatures lower than 800 K, the measured

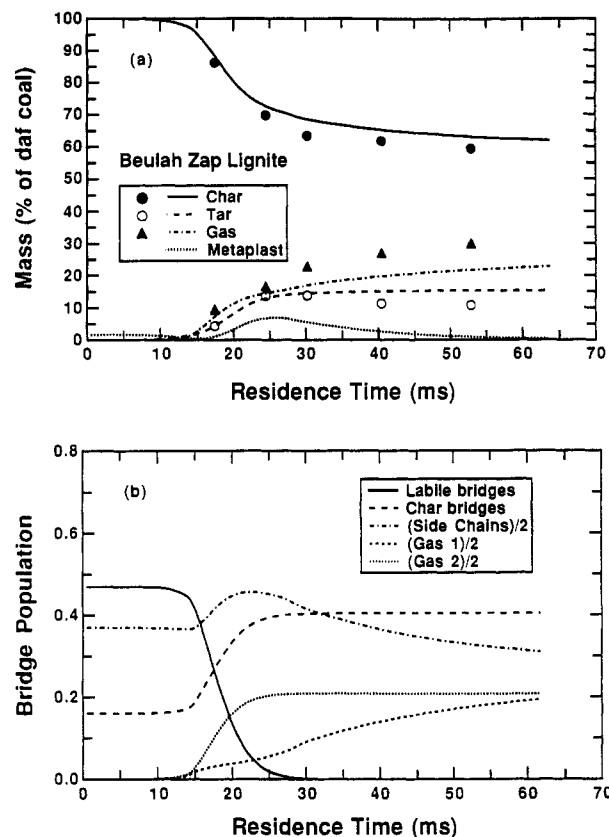


Figure 7. (a) CPD calculations of devolatilization yields of char, tar, and light gases versus time for North Dakota Beulah Zap lignite. Experimental data are from Serio et al.,⁸ and chemical structure parameters for the model are taken directly from NMR (one adjustable parameter: c_0). (b) Bridge dynamic population parameters on a per site basis as a function of time (δ , g_1 , and g_2 variables are divided by 2).

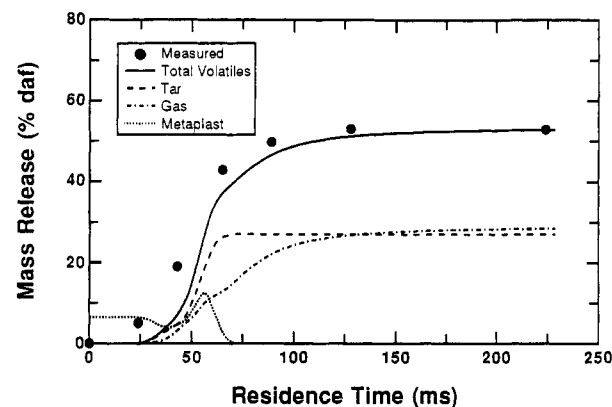


Figure 8. CPD model predictions (curves) of devolatilization yields of char, tar, and light gases versus time for Illinois No. 6 coal in the Sandia CDL. Experimental data (points) are from Fletcher;^{44,45} and chemical structure parameters for the model are taken directly from NMR data (no adjustable parameters).

mass release at 1 K/s exhibits the same temperature dependence as the measured mass release at 1000 K/s with the 30-s hold. The initial mass release at 1000 K/s with no hold time at the peak temperature occurs at temperatures that are approximately 150 K higher than in the 30-s hold time experiment. The high-temperature volatiles yield for the 1 K/s experiment was about 7% (daf) lower than in the 1000 K/s experiments.

An earlier version of the CPD model¹⁹ showed good agreement with the temperature dependence and total volatiles yields measured by Gibbins-Matham and Kandiyoti.⁴⁶ Since the cross-linking rate affects the total yield

(46) Gibbins-Matham, J.; Kandiyoti, R. *Energy Fuels* 1988, 2, 505.

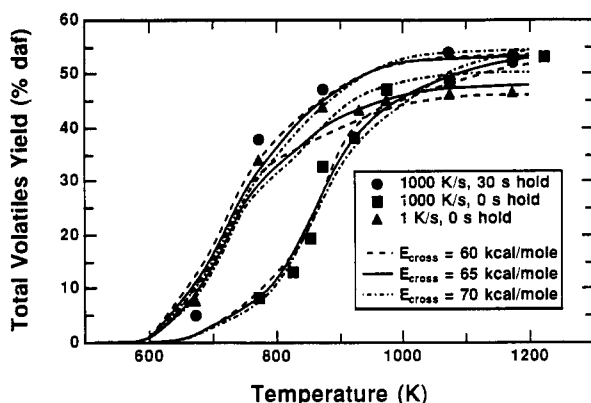


Figure 9. CPD model predictions of total volatiles yields (curves) with different values of E_{cross} compared with the heated grid data (points) of Gibbins-Matham and Kandiyoti⁴⁶ for a Pittsburgh No. 8 coal at different heating rates.

as a function of heating rate, these data were used to help select values of E_{cross} for the improved CPD model. Comparisons with these data using the improved version of the CPD, with the three different values of E_{cross} , are shown in Figure 9. Chemical structure parameters for these predictions are derived from the tar and total volatiles yields at 1000 K/s with 30-s hold at 973 K (i.e., values for \mathcal{E}_0 were adjusted to fit this data point for each value of E_{cross}). The predictions show only a slight sensitivity to the value for E_{cross} . For example, in the 1000 K/s case with 0-s hold time, predicted total yields at 1200 K range from 50 to 53%. The predictions of total volatiles yields using $E_{\text{cross}} = 70$ kcal/mol at 1 K/s are approximately 5% higher than the data at high temperatures (above 900 K). The value of E_{cross} of 65 kcal/mol seems to give slightly better agreement with the data in these three cases than the other two values. The relative insensitivity of the predictions to the value of E_{cross} is most likely due to the moderate temperatures (1200 K maximum) in these heated grid experiments, which limits the cross-linking rate.

Pyridine Extract Data. Fong and co-workers³⁸ measured the pyridine extract yields from chars produced during devolatilization experiments as a function of residence time on a heated screen at heating rates of ~ 500 K/s. The extract yield is related to the amount of finite material (metaplast) in the char at any time. Approximately 25% of the parent bituminous coal was extracted with pyridine, and up to 65% of the parent coal appeared as extract yield during pyrolysis. However, after completion of pyrolysis, extract yields of 0% were measured.

Only qualitative comparisons of CPD model predictions can be made with the data from Fong et al.³⁸ because pyridine extracts colloidal material (with molecular weights of several million amu) as well as metaplast that may never vaporize at typical pyrolysis conditions. The experimental extraction procedure was performed at the boiling point of pyridine (388.5 K), which may also have broken some of the weak bonds in the coal and chars. Extraction experiments performed with other solvents, such as tetrahydrofuran (THF), typically give lower extract yields ($\sim 10\%$ or less). In addition, the mass release predicted by the CPD model occurs at residence times 10% earlier than measured by Fong and co-workers. The particle temperature histories determined in this experiment may be subject to well-known biases that commonly occur in heated-screen temperature measurements.⁴⁴⁻⁴⁸ The mass

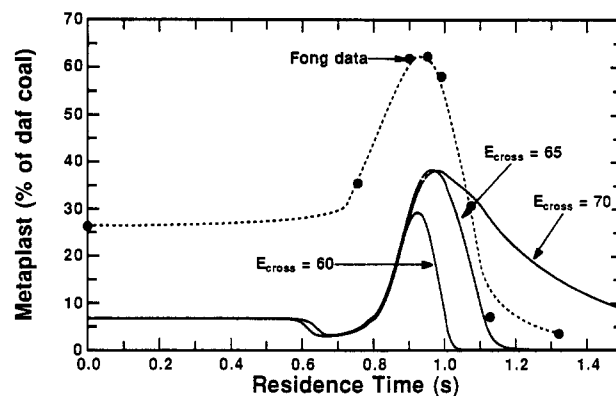


Figure 10. CPD model predictions (solid curves) of the amount of metaplast in a char particle derived from a Pittsburgh No. 8 coal, compared with pyridine extract data (points and dashed line) from a heated grid experiment.³⁸ In both the experiment and the calculations, the heating rate is 640 K/s, with a final holding temperature of 1018 K.

release predicted by the CPD model agrees with experimental data at rapid heating rates where particle temperatures have been measured optically^{8,19,45} and with data at low heating rates (1 K/s), as explained above.

The predicted amounts of metaplast for the Fong experiment (case D in his experiment) with a heating rate of 640 K/s and a final temperature of 1018 K are shown in Figure 10 as a function of residence time for different values of E_{cross} , along with the pyridine extract yield data. The chemical structure and rate parameters used in these predictions are identical to those used in the predictions described in the previous section for the data of Gibbins-Matham and Kandiyoti.⁴⁶ The predictions show production and depletion of metaplast in the same time period that the increase in pyridine extracts occurs. As mentioned above, the predicted amount of metaplast is not expected to agree because pyridine extracts contain significant amounts of colloidal dispersions. The predictions with E_{cross} equal to 60 and 65 kcal/mol are in qualitative agreement with the residence times of the peak in the extract yield data. The prediction using $E_{\text{cross}} = 70$ kcal/mol exhibits a long tail in the final stages of metaplast depletion (residence times between 1 and 1.5 s), whereas a rapid depletion of the extract yields are observed at a residence time of 1.1 s. The best agreement between CPD model calculations and the pyridine extract data is achieved using $E_{\text{cross}} = 65$ kcal/mol.

NMR Data. Previous measurements of the chemical structure of char particles sampled as a function of residence time in an entrained flow reactor at Sandia identify quantitatively the number of bridges and loops between aromatic clusters.^{41,42} The number of bridges and loops per cluster is a quantitative indication of the extent of cross-linking in the solid material. For an Illinois No. 6 bituminous coal, the number of bridges and loops per cluster was shown to increase in the late stages of devolatilization after the tar was released.^{41,42} For a North Dakota Beulah Zap lignite, the number of bridges and loops per cluster increased early in the devolatilization process.⁴² In the improved CPD model, the amount of metaplast that has been reattached to the infinite char matrix is calculated, providing a direct measure of the extent of cross-linking. Model calculations of the amount of reattached metaplast are therefore compared with the number of bridges and loops per cluster determined from NMR analyses of char samples. Heating rates in these experiments are approximately 10^4 K/s, with a maximum gas temperature of 1250 K and a maximum particle tem-

(47) Freihaut, J. D.; Proscia, W. M. *Energy Fuels* 1989, 3, 625.

(48) Solomon, P. R.; Serio, M. A.; Carangelo, R. M.; Markham, J. R. *Fuel* 1986, 65, 182.

Table III. Chemical Structure Parameters from ^{13}C NMR for 19 Coals^a

coal type	%C (daf)	M_{clust}	m_a	P_0	f_a'	AC/Cl	$\sigma + 1$
Zap (AR)	72.9	277	40	0.63	0.55	9	3.9
Wyodak (AR)	75.0	410	42	0.55	0.55	14	5.6
Utah (AR)	80.7	359	36	0.49	0.61	15	5.1
Ill6 (AR)	77.7	316	27	0.63	0.72	15	5.0
Pitt8 (AR)	83.2	294	24	0.62	0.70	15	4.5
Stockton (AR)	82.6	275	20	0.69	0.75	14	4.8
Freeport (AR)	85.5	302	17	0.67	0.81	18	5.3
Pocahontas (AR)	91.1	299	14	0.74	0.86	20	4.4
Zap (Sandia)	66.6	410	51	0.59	0.57	14	5.2
Zap (Sandia)	66.6	440	52	0.48	0.57	13	5.0
Blue (Sandia)	75.6	410	47	0.42	0.53	14	5.0
Ill6 (Sandia)	74.1	270	34	0.56	0.67	11	4.1
Pitt8 (Sandia)	84.2	356	34	0.45	0.60	15	5.0
Poc (Sandia)	88.8	316	18	0.70	0.77	18	4.0
Zap (AFR)	66.5	339	46	0.63	0.58	11	4.5
Rose (AFR)	72.4	459	48	0.57	0.53	15	5.8
Ill6 (AFR)	73.6	267	29	0.61	0.67	11	4.6
1443 (lig, ACERC)	72.3	297	36	0.59	0.56	10	4.8
1488 (sub, ACERC)	76.0	310	37	0.54	0.56	11	4.7
1468 (anth, ACERC)	95.4	656	12	0.89	0.94	49	4.7

^a AR refers to eight coals from the Argonne premium sample bank;^{15,49} Sandia refers to five coals examined at Sandia National Laboratories by Fletcher;⁵⁰ AFR refers to three coals examined by Serio et al.⁸ at Advanced Fuel Research (AFR); ACERC refers to three coals examined from the Advanced Combustion Engineering Research Center (ACERC) at BYU and the University of Utah.⁵¹

perature of 1200 K. The actual particle temperature history is determined from measurements of the size, temperature, and velocity of individual particles at different residence times in the entrained flow reactor.^{44,45} As shown in Figure 11 for an Illinois No. 6 bituminous coal, the model predicts that the amount of reattached metaplast remains constant until the late stages of mass release and then increases rapidly, which agrees qualitatively with the extent of mass release at which the measured increase in the number of bridges and loops per cluster is observed. The prediction with E_{cross} equal to 70 kcal/mol shows the latest rise in the amount of reattached metaplast, which agrees better with the NMR data than the predictions using the two lower values of E_{cross} . The uncertainties involved in these NMR data are sufficiently large, however, that only $E_{\text{cross}} = 60$ kcal/mol can be considered to be an unlikely value.

On the basis of the comparisons with (i) pyridine extract data, (ii) total volatiles yields as a function of heating rate, and (iii) NMR determinations, a value of $E_{\text{cross}} = 65$ kcal/mol was selected for use in the CPD model. All calculations presented in the remainder of this paper use $E_{\text{cross}} = 65$ kcal/mol.

(c) **Chemical Structure Parameters.** The pyrolysis behavior of different coals, including product yields and release rates, is directly a function of the chemical structure of the coal. Ideally, all of the input parameters for a coal pyrolysis model should be determined from measurements of the elemental composition and chemical structure as a function of coal type. It is quite possible that sophisticated devolatilization models may be able to fit tar and gas yields, and even molecular weights, based on physically unrealistic values of chemical structure parameters. These models often have enough adjustable parameters that the physical interpretation of individual parameters becomes difficult, although in all cases "the model agrees well with the data". Such was the case with earlier formulations of the CPD model; input parameters were determined from curve-fits of tar and total volatiles yields, even though the processes of vapor-liquid equilibrium and cross-linking were not treated.^{9,19} In the present formulation of the CPD model, five parameters describe the chemical structure of each coal: (i) the coordination number, $\sigma + 1$, (ii) the initial number of intact labile bridges \mathcal{L}_0 ; (iii) the initial number of char bridges c_0 ; (iv) the hypothetical ultimate gas yield

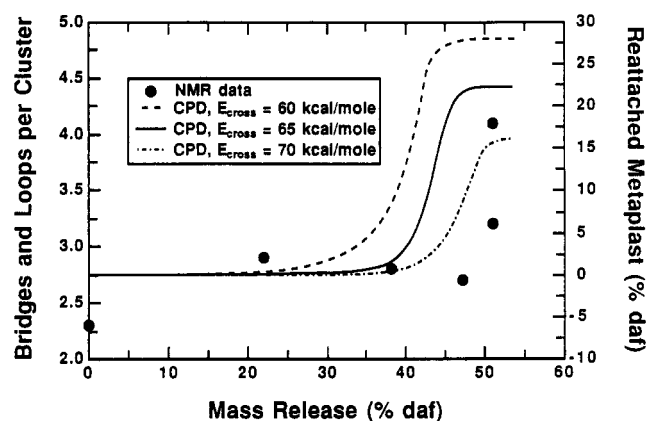


Figure 11. CPD model predictions (with different values of E_{cross}) of the amount of reattachment of metaplast in a char derived from an Illinois No. 6 coal, compared with NMR data from an entrained flow reactor.⁴¹

$f_{\text{gas},\infty}$; (v) the average molecular weight of an aromatic cluster m_a (this parameter was simply set to 120 amu in the original treatment of the CPD model). The approach taken here is to take the input parameters in the CPD model directly from the NMR determinations of chemical structure, which drastically reduces the number of adjustable parameters in the model.

The coordination number ($\sigma + 1$) is taken directly from ^{13}C NMR measurements of the parent coals using techniques described by Solum and co-workers.¹⁵ Since the coordination number is defined as the total number of attachments per cluster, it accounts for side chains as well as labile and char bridges. Measured values of the coordination number range from 3.9 to 5.8 but show no systematic variation with coal rank, as shown in Figure 12 for 19 coals: the 8 Argonne premium coals;⁴⁹ 5 research coals used at Sandia National Laboratories;⁵⁰ 3 research coals used at Advanced Fuel Research (AFR);⁸ 3 coals from the ACERC suite.⁵¹ Relevant chemical structure data for

(49) Vorres, K. S. Users' Handbook for the Argonne Premium Coal Sample Bank, 1989; Argonne National Laboratory, supported by DOE contract W-31-109-ENG-38. Also: Vorres, K. S. ACS Div. Fuel Chem. Prepr. 1987, 32:4, 221.

(50) Fletcher, T. H.; Hardesty, D. R. Compilation of Sandia Coal Devolatilization Data: Milestone Report. Contract Report for DOE's Pittsburgh Energy Technology Center, contract FWP 0709, in press.

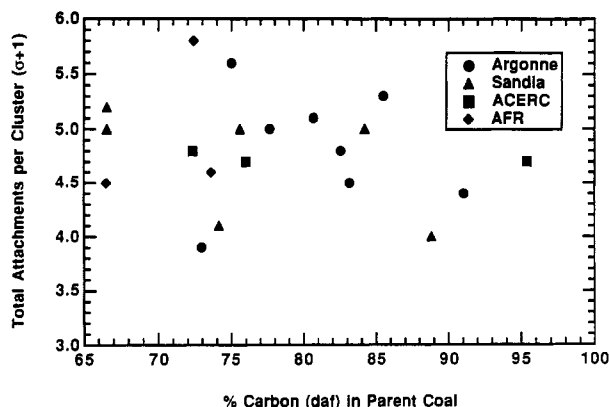


Figure 12. Total number of attachments per aromatic cluster ($\sigma + 1$) determined from ^{13}C NMR analyses. NMR data are for coals from the Argonne premium sample bank^{15,49} from AFR,⁸ and from the Penn State sample bank examined at Sandia^{41,42,50} and at BYU (ACERC).⁵¹

these coals, using techniques discussed by Solum and co-workers,¹⁵ are shown in Table III. The chemical structure data are discussed in this section, since the data have appeared separately in several publications.

The highest values of the coordination number occur for the Rosebud subbituminous coal from AFR and for the Wyodak coal from the Argonne premium sample bank. The Rosebud subbituminous coal sample analyzed by NMR spectroscopy was unfortunately subjected to oxidation over long times at room temperatures (weathering), which may have caused structural changes in the coal. The corresponding number for the Wyodak subbituminous coal, which is similar to the Rosebud coal, is 5.6. This may indicate a peculiar feature of subbituminous coals which is not completely understood at present. The coordination number has been shown to stay relatively constant in coal chars during devolatilization.^{41,42} The distribution of attachments between side chains versus the bridges and loops per cluster, however, does change as a function of the extent of devolatilization, dependent on coal type.^{41,42} The coordination number ($\sigma + 1$) can be used to calculate the number of intact bridges per cluster (α) used by Solomon^{18,52} as follows: $\alpha = p(\sigma + 1)/2$. The value of α , measuring the number of intact bridges to clusters, is greater than 2 but less than the value of 4–5 for the coordination number ($\sigma + 1$), since the coordination number accounts for side chains as well as bridges.

The population of intact bridges in the parent coal (p_0) is also measured by ^{13}C NMR and is used as an input parameter in the CPD model, noting that $p_0 = \mathcal{L}_0 + c_0$. The value of p_0 therefore sets an upper bound to the number of labile bridges \mathcal{L}_0 in the parent coal, while c_0 determines the actual fraction of the total bridges that are stable at temperatures typical of devolatilization. There seems to be no consistent variation in the measured value of p_0 as a function of coal rank, as shown in Figure 13, except for the fact that the anthracite has more intact bridges than the other coals. The scatter in these data is interpreted as diversity in coals of similar rank and indicates more diversity among low rank coals than high rank coals. The value of c_0 is related to the concentration of stable bridges between clusters, such as biaryl and aryl-ether linkages, particularly in the high rank coals. There is currently no method to measure this quantity, and c_0 is determined empirically by comparing CPD model predictions with measured tar yields. In low-rank coals

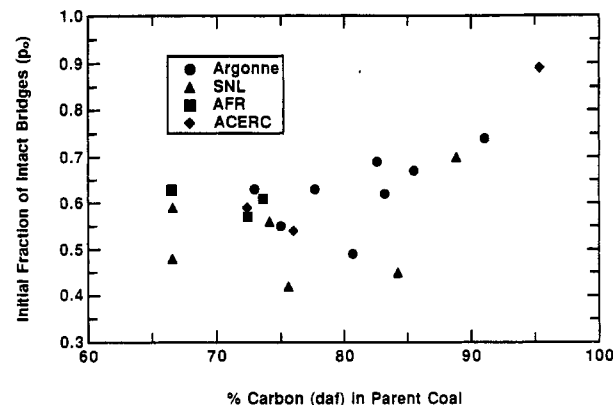


Figure 13. Initial fraction of intact bridges p_0 determined from ^{13}C NMR analyses. NMR data are for coals from the Argonne premium sample bank^{15,49} from AFR,⁸ and from the Penn State sample bank examined at Sandia^{41,42,50} and at BYU (ACERC).⁵¹

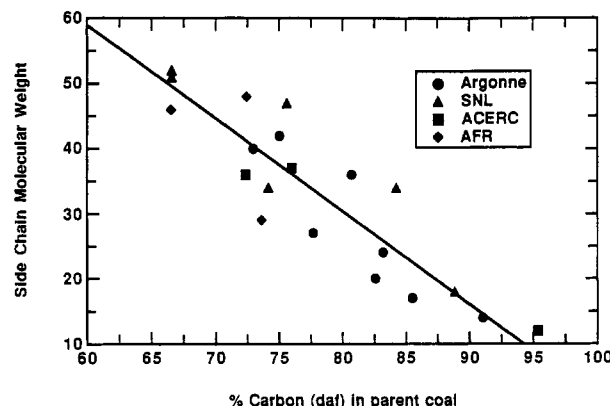


Figure 14. Measured molecular weights per side chain m_s determined from ^{13}C NMR analyses. NMR data are for coals from the Argonne premium sample bank^{15,49} from AFR,⁸ and from the Penn State sample bank examined at Sandia^{41,42,50} and at BYU (ACERC).⁵¹ The line represents a correlation of the data.

(particularly lignites), c_0 is used to approximate the early cross-linking that occurs. The introduction of a progressive cross-linking mechanism into the CPD formulation is the subject of ongoing research and will eliminate the need to specify c_0 for low rank coals.

The value of $f_{\text{gas},\infty}$ is related to the molecular weight of labile bridges (m_b), the molecular weight of the aromatic part of the cluster (m_a), the initial char bridge population (c_0), and the coordination number ($\sigma + 1$), as follows:⁹

$$f_{\text{gas},\infty} = \frac{m_b(\sigma + 1)(1 - c_0)}{[2m_a + m_b(\sigma + 1)(1 - c_0)]} \quad (22)$$

The average molecular weight of a labile bridge in the CPD model is twice the molecular weight of a side chain ($m_b = 2m_s$). The value of m_s can be estimated from the ^{13}C NMR data by subtracting the mass of the aromatic material from the total cluster molecular weight and dividing by the number of attachments per cluster, as follows:

$$m_b = \frac{M_{\text{clust}} - C_{\text{clust}} M_C}{\sigma + 1} \quad (23)$$

In the NMR estimates, the high-rank coals have low side chain molecular weights compared to the low rank coals, as shown in Figure 14. This means that the Pocahontas is a compact, highly aromatic coal, with a large number of intact bridges between aromatic clusters that are smaller than bridges observed in lower rank coals. The low rank coals contain approximately the same number of bridges per cluster, but the molecular weight of each bridge is

(51) Smith, K. L.; Smoot, L. D. *Prog. Energy Combust. Sci.* **1990**, *16*, 1.

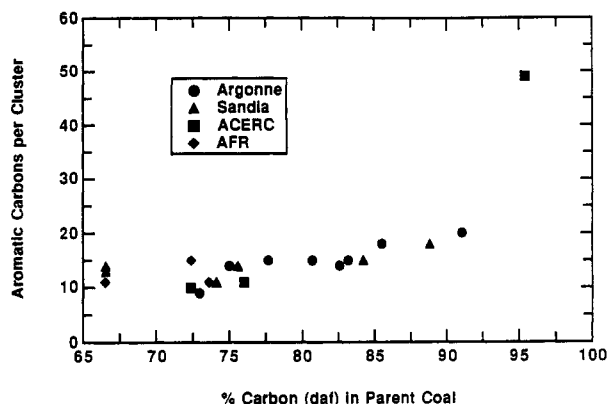


Figure 15. ^{13}C NMR determinations of the average number of aromatic carbons per cluster as a function of the carbon content of the parent coal. NMR data are for coals from the Argonne premium sample bank^{15,49} from AFR,⁸ and from the Penn State sample bank examined at Sandia^{41,42,50} and at BYU (ACERC).⁵¹

higher. These trends correspond to measured aromaticities as a function of coal rank; high-rank coals exhibit higher carbon aromaticities (and hence less aliphatic carbon) than low-rank coals. The larger aliphatic bridges in the low-rank coals are sometimes referred to as polymethylenes.⁵² The NMR data are consistent with the observation that more aliphatic $-\text{CH}_2-$ (polymethylene) is seen in FTIR spectra of low rank coal tars than in high rank coal tars.³⁶

Realistically, an unspecified fraction of tightly bound α -methyl groups remain attached the aromatic unit at typical devolatilization temperatures. These α -methyl groups are counted in the NMR measurements as side chains but should be considered as part of the aromatic cluster in the CPD model, since they are not released during devolatilization. The fraction of tightly bound side chains may be a significant quantity in high-rank coals, such as the low-volatile bituminous Pocahontas coal, where side-chain molecular weights are small to begin with. Good agreement with gas yield data from Pocahontas coal was achieved when the side-chain molecular weight used in the CPD model was reduced by 7 amu from the NMR measurements ($m_s = 14$ as measured by NMR, so $m_s' = 7$ in the CPD model for this coal). This factor of 7 amu reduction in the NMR-measured value of m_s was also used for all other coals; this factor becomes less important for lower rank coals because the m_s is larger, reaching 52 amu for the Zap lignite from the PETC suite (PSOC-1507D).

The average molecular weight of an aromatic cluster (M_{clust} , as measured by Solum and co-workers¹⁵) consists of contributions by aromatic and aliphatic moieties. The molecular weight of each fragment size bin ($m_{\text{frag},n}$) in the CPD model is calculated from eq 2.⁹ This equation is a nonlinear function of the number of aromatic clusters per fragment (n), the number of intact bridges ($p = \mathcal{L} + c$), and the number of side chains (δ). The molecular weight of a dimer is therefore not simply twice the molecular weight of a monomer, etc. The average molecular weight of an aromatic cluster, including the side chains and half of the bridges, has also been estimated by Solum et al.¹⁵ using NMR measurements of coal structure. The molecular weight per cluster is calculated from the ratio of the number of aromatic carbons per cluster to the carbon aromaticity, as follows:

$$M_{\text{clust}} = \frac{C_{\text{clust}} M_c}{f_a' x_C} \quad (24)$$

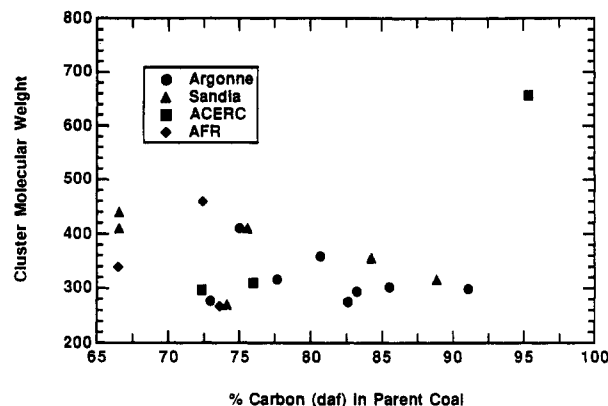


Figure 16. Measured average molecular weights per aromatic cluster M_{clust} determined from ^{13}C NMR analyses. NMR data are for coals from the Argonne premium sample bank^{15,49} from AFR,⁸ and from the Penn State sample bank examined at Sandia^{41,42,50} and at BYU (ACERC).⁵¹

where M_{clust} is the molecular weight per cluster, C_{clust} is the number of aromatic carbons per cluster, M_c is the molecular weight of carbon (12 amu), f_a' is the carbon aromaticity, and x_C is the percentage of carbon in the coal (daf basis). The number of aromatic carbons per cluster increases uniformly with rank, as shown in Figure 15. However, the NMR determinations of cluster molecular weight show no such clear trend as a function of coal rank, due to diversity in chemical structure; only a slight trend is observed that M_{clust} decreases slightly as rank increases, as shown in Figure 16.

Knowing the molecular weight per cluster M_{clust} , the side-chain molecular weight m_s , and the coordination number $\sigma + 1$, the average molecular weight of the aromatic part of the cluster (m_a) is determined in the CPD model by rearranging eq 23, as follows:

$$m_a = M_{\text{clust}} - m_s(\sigma + 1) \quad (25)$$

This equation ensures that the mass associated with α -carbons is assigned to m_a when the measured value of m_s is reduced by 7 amu, as described above. Equation 25 ensures that the molecular weight of a monomer fragment, as predicted by eq 2 with $n = 1$, will be equal to the cluster molecular weight M_{clust} from the NMR data.

The extensive use of NMR data for input parameters limits the amount of curve-fitting that is possible with the CPD model, and calculations become true predictions rather than empirical interpolations. As discussed above, the only adjustable coal structure parameter is the initial population of char bridges c_0 , which in effect limits the tar production from the labile bridges. This empiricism for low rank coals will be eliminated by the introduction of a progressive cross-linking mechanism in the CPD model, as discussed by Solomon and co-workers.⁵²

The tar yields predicted by the CPD model are limited principally by the values of the coordination number $\sigma + 1$ and the initial bridge population p_0 . The gas yield is principally affected by the value of $f_{\text{gas},\infty}$, which is calculated directly from the average molecular weight per side chain m_s determined in the NMR measurements. The value of c_0 limits the tar yield in the low rank coals (approximating early cross-linking) and in the high-rank coals (due to finite populations of char bridges thought to exist in the parent coal matrix). The CPD calculations of tar and total volatiles yields for the high volatile bituminous coals, with $c_0 = 0$, become true predictions based on NMR parameters. Only one coal-dependent parameter is currently used in the CPD calculations for the low or high rank coals, meaning that the total volatiles yield is a true

(52) Solomon, P. R.; Fletcher, T. H.; Pugmire, R. J. *Proceedings of the Pittsburgh Coal Conference*; Pittsburgh, 1990; p 3.

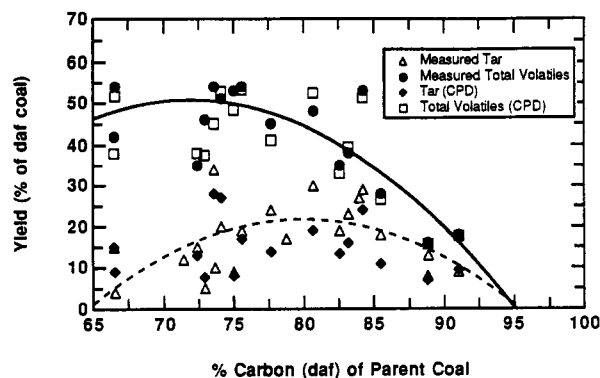


Figure 17. Comparison of predicted and measured tar and total volatiles yields for a wide range of coals. Carbon content is used to illustrate coal rank. Data are for coals from the Argonne premium sample bank,^{15,49} from AFR,⁸ and from the Penn State sample bank^{41,42,50,51} for which NMR data are available.

prediction while the calculated tar yield is affected by c_0 .

Comparison with Data

(a) Tar and Total Volatiles Yields. Since coal-dependent chemical structure parameters for the CPD model are taken directly from NMR data, with only one adjustable parameter as explained above, predictions of tar and total volatiles yields are compared with measured yields in order to evaluate the model. Predicted tar molecular weights are also compared with available data as part of the model evaluation. The predictions of pyrolysis behavior for the high volatile bituminous coals have no adjustable parameters, since $c_0 = 0.0$ for these coals. For example, the comparisons of CPD model predictions with bituminous coal data shown in Figures 5 and 8 were performed with no adjustable parameters (all chemical structure parameters taken directly from NMR data), while the comparisons shown in Figures 6 and 7 used only c_0 as an adjustable parameter. This method of model evaluation is in contrast to the more common route of setting the parameters to exactly match the yields and molecular weights, and then rationalizing the coefficients based on known structure.

The predictions shown in Figures 5–8 show the relationships between tar release, metaplast formation, cross-linking, and gas release. In each case, the metaplast decreases slightly during the initial stages of tar release, corresponding to the release of finite fragments present in the parent coal. This is followed by labile bridge scission, generating more finite fragments which are distributed between tar and metaplast. Labile bridge scission also generates additional side chains, and a net decrease in side chains to light gas release is not seen until the end of labile bridge scission. The mass fraction of metaplast slowly decreases to zero after tar release due to cross-linking. A significant population of side chains exists at the end of these predictions. The plots of the bridge population parameters (Figures 5b, 6b, and 7b) account for bridges and side chains released with the tar (in a manner similar to eq 21) but do not account for side chains removed during the cross-linking process. However, significant side-chain populations are observed in ¹³C NMR analyses of chars from the Sandia experiments,⁵⁰ which is consistent with CPD model predictions. The distribution of the activation energy for light gas release allows gradual release of side chains as light gas as the particle temperature is increased.

CPD model predictions of tar and total volatiles yields are compared with several sets of data in Figures 17 and 18. The data shown here were obtained (a) at low heating

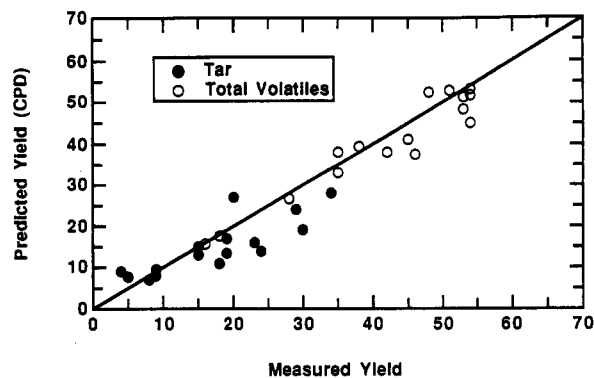


Figure 18. Comparison of predicted and measured tar and total volatiles yields for a wide range of coals. The 45° line illustrates the difference between the predicted and measured values. Data are for coals from the Argonne premium sample bank,^{15,49} from AFR,⁸ and from the Penn State sample bank^{41,42,50,51} for which NMR data are available.

rates in a TGA⁵³ for the eight Argonne premium coal samples, (b) in rapid heating experiments for three coals in a heated tube reactor,⁸ and in a laminar flow reactor for five coals at heating rates of approximately 10 K/s.^{45,50} The tar yields in the TGA were obtained by an FTIR technique, changing the absorbance as a function of coal type. Only the maximum tar yields reported in the rapid heating experiments are used (based on mass balances), since the tar reacts further in the hot reactor gases. The tar yields are estimated to be accurate only to within $\pm 5\%$, due to errors in mass balances and/or absorbance values.

The general trend shown in Figure 17 is that the low-rank coals (65–75% carbon) attain the same total volatiles yields as the high volatile bituminous coals (80–85% carbon), and then the total volatiles yields decrease for the high rank coals (>85% carbon). The tar yields are generally small for the low-rank coals, reach a maximum for the high volatile bituminous coals, and then decrease for the high rank coals. However, these general trends (indicated by the curves in Figure 17) are not universal, and there is considerable scatter in the data. The comparison of predicted tar and total volatiles yields (Figure 18) shows that the CPD model does not merely predict a trend but rather gives quantitative agreement, even though input parameters were taken directly from NMR characterizations of coal structure. The tar yield is slightly underpredicted for high tar yields (i.e., high volatile bituminous coals) but is probably within the uncertainty in the data.

The amount of finite fragments that exist in the parent coal is a function of the initial bridge population parameters (\mathcal{L}_0 and c_0) and the coordination number ($\sigma + 1$). At ambient temperatures, the vapor pressure of the finite fragments is much lower than the ambient pressure, and the initial finite fragments exist in the coal as metaplast. The fraction of the parent coal that exist as metaplast ($f_{\text{meta},0}$) calculated in the CPD model using the input parameters from NMR data, varies from 0.3% of the daf coal for the Pocahontas low volatile bituminous coal from the Argonne premium sample bank to 13% for the New Mexico Blue subbituminous coal (PSOC-1445D). Intermediate values of $f_{\text{meta},0}$ were determined for the other coals, although there is no clear distinction with coal rank. In general, the value of $f_{\text{meta},0}$ was lower for the Argonne coals, with a maximum of 4.9% for the Utah Blind Canyon high volatile bituminous coal. Solvents such as pyridine produce extract yields from bituminous coals as high as

(53) Solomon, M. A.; Serio, M. A.; Carangelo, R. M.; Basilakis, R.; Gravel, D.; Baillargeon, M.; Baudais, F.; Vail, G. *Energy Fuels* 1990, 4, 319.

25%,^{38,54} but contain significant amounts of colloidal dispersions.⁵⁵ Other coal devolatilization models^{11,14} use pyridine extract yields as a measure of the initial amount of metaplast. The initial fraction of metaplast in the CPD model, however, correlates with extract yields using moderate solvents with moderate contact times, such as tetrahydrofuran, where less colloidal dispersions are generally obtained than with pyridine. For instance, an extract yield of approximately 6% was obtained by soaking a Pittsburgh seam coal in tetrahydrofuran at room temperature for 1 h, followed by a 15-min ultrasonic bath which raised the THF nearly to its boiling point.²⁵ Recent extraction experiments by Lee and co-workers,⁵⁶ performed in a Soxhlet apparatus for 48 hours, indicate low extract yields for Zap lignite and Pocahontas coal (2 and 1%, respectively) and moderate extract yields for high volatile Illinois No. 6 and Utah Blind Canyon coals (17 and 19%, respectively). At present, no attempt is made in the CPD model to derive input parameters from the extract yield data, since the degree of chemical interaction between the coal and the solvent is uncertain. The examination of solvent extract yields in pyridine and in THF, with relation to the CPD model and other network models, is currently the subject of ongoing research.

(b) Tar Molecular Weight. The experimental measurement of tar molecular weight distributions is a challenging and controversial research topic. Size exclusion chromatography (SEC) and high-performance liquid chromatography (HPLC) have both been used to analyze coal tars but suffer from the difficulty in selecting calibration compounds with the same conformational geometries as exist in coal tars. Freihaut and co-workers³⁶ showed that large differences in the average tar molecular weight occur when the standard polystyrene calibration is used in SEC analyses rather than more realistic model compounds.

Another technique commonly used to determine tar molecular weights is field ionization mass spectrometry (FIMS). Relative structure differences in the tars from the eight Argonne premium coals at slow heating rates (0.05 K/s) were recently analyzed using FIMS.⁴⁰ Molecular weight distributions were also determined for tars from a lignite at two additional heating rates (600 and 20 000 K/s). However, in the FIMS technique, it is difficult to determine the percentage of the sample that is transported through the transfer lines to the mass spectrometer; the small transfer lines may act as chromatographic columns and absorb large and/or irregularly shaped compounds. As in the liquid chromatographic techniques, this method is viewed as a measure of trends in tar molecular weight distributions and cannot be used quantitatively with great confidence.

Comparisons of trends in the calculated and measured distributions help determine if the coal structure and chemical reaction chemistry is described appropriately. In the CPD model, tar consists of a distribution of fragment sizes, and these are averaged on a mass basis. The smallest fragment size bin in the model is the average monomer molecular weight taken from NMR data and hence relatively coarse size bins are used in the model. For this reason, comparisons of mass-averaged or number-averaged tar molecular weights are used to evaluate model performance. The mass-averaged tar molecular weights cal-

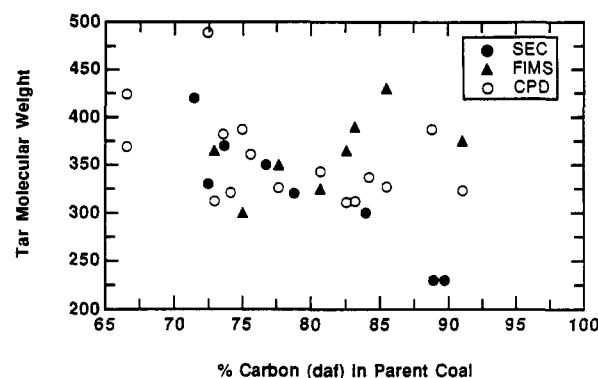


Figure 19. Mass-averaged molecular weights of tars from different coals calculated by the CPD model compared with SEC data from Freihaut et al.³⁶ and FIMS data from Solomon, et al.⁴⁰ The CPD calculations were performed for rapid heating rates ($\sim 10^4$ K/s), and the FIMS tar data for lignite are from the rapid heating experiment.

culated from the CPD model are compared with SEC data from Freihaut et al.³⁶ and FIMS data from Solomon et al.⁴⁰ in Figure 19. The carbon content is used here to approximate coal rank, in order to directly compare with the data from Freihaut and co-workers. The average tar molecular weights shown for the FIMS data were estimated by visual inspection of the spectra and hence may be in error by approximately 50 amu. The CPD calculations were performed for rapid heating rates ($\sim 10^3$ – 10^4 K/s), except for the Pocahontas low volatile bituminous coal. The FIMS tar data for lignite in this comparison are from the rapid heating experiment (2×10^4 K/s). The SEC data shown here are from Freihaut's "model compound calibration"; his data from the polystyrene calibration are 400–500 amu higher and are not thought to be realistic. All of the SEC data were obtained at heating rates estimated at 2000–5000 K/s in an estimated flow reactor where thermal radiation, rather than convection, was the dominant mode of particle heating.

The disagreement between the FIMS and the SEC tar molecular weight data is indicative of the quantitative and qualitative uncertainties in the two techniques. The high-rank coal tars exhibit higher average molecular weights than the low-rank coal tars in the FIMS data, while the SEC data indicate the opposite trend (low-rank tars have higher average molecular weights). The CPD model predictions of average tar molecular weight show no clear trend as a function of coal rank, although a linear regression would indicate a slight decrease in tar molecular weight as rank increases. The most important conclusion from this comparison is that CPD model predictions of the average tar molecular weights from different coals, using NMR parameters as input data, are within 100 amu of both the FIMS and SEC data. Considering the uncertainty in the measurements, the overall qualitative and quantitative agreement between the predicted and measured average tar molecular weights is reasonable.

There is considerable uncertainty in measured tar molecular weight distributions as well as average molecular weights. For this reason, a direct comparison of predicted and measured tar molecular weight distributions seems unwarranted here. In general, at atmospheric pressure under typical devolatilization conditions, the CPD model predicts that all monomers and most dimers have sufficient vapor pressure to become tar. Only a very small amount higher molecular weight fragments vaporizes. Approximately 60% of the fragments generated from a lattice with coordination numbers of 4–5 are monomers. With measured cluster molecular weights of coals in the range

(54) Berkowitz, N. *The Chemistry of Coal*; Elsevier: New York, 1985; Vol. 7, pp 40–41.

(55) *Ibid.*, p 283.

(56) Carlson, R. E.; Critchfield, S.; Vorkink, W. P.; Dong, J.-Z.; Pugmire, R. J.; Bartle, K. D.; Lee, M. L.; Zhang, Y.; Shabtai, J. *Fuel* 1992, 71, 19.

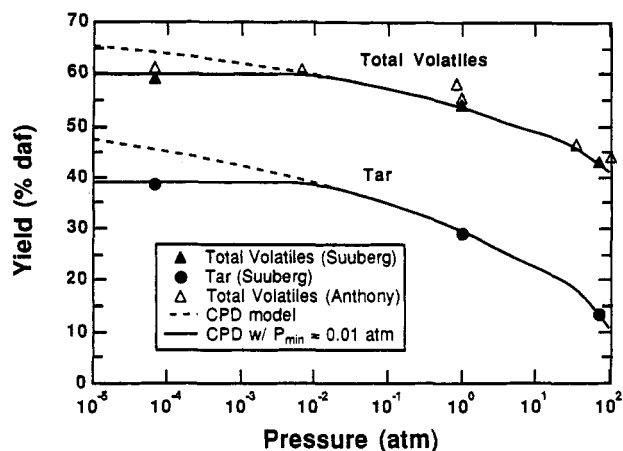


Figure 20. Comparison of CPD model predictions (curves) with pressure-dependent tar and total volatiles yield data (points) from Anthony⁵⁷ and Suuberg et al.³² for bituminous coals. Dashed lines represent predictions with no minimum internal particle pressure; solid lines represent predictions with a minimum internal pressure of 0.01 atm.

250–450 (Figure 16), this means that the molecular weight of atmospheric tar drops significantly between dimers and trimers, or in the range 750–1000 amu. This cutoff range is similar to that observed in FIMS data.⁴⁰ The qualitative agreement in molecular weight distributions is consistent with the general agreement in average tar molecular weights shown in Figure 19.

(c) Pressure Effects. Comparisons between predictions made with the CPD model and experimental measurements performed as a function of pressure are presented in Figure 20. Data are from heated grid experiments by Anthony⁵⁷ and by Suuberg and co-workers³² for a Pittsburgh No. 8 bituminous coal; very little data other than these have been collected as a function of pressure. Particle heating rates in these experiments were approximately 1000 K/s for the Suuberg data and 700 K/s for the Anthony data, with a final temperature of 1273 K and hold times ranging from 2 to 10 s. Rate data from these early heated grid experiments are subject to questions regarding the validity of the particle temperature during the heating time.^{44–47} The uncertainties in particle temperature during heating do not significantly affect the yield data for the long hold time experiments. Model predictions were made with a heating rate of 1000 K/s and a 5-s hold time at 1273 K using the chemical structure coefficients for a Pittsburgh No. 8 coal, with slight adjustments made to match the tar and total volatiles yield data at 1 atm.

The dashed line in Figure 20 represents the predicted yield if there is no pressure drop inside the particle, whereas the solid line represents a minimum internal particle pressure P_{\min} of 0.01 atm. A minimum internal particle pressure of 0.2 atm was used by Solomon and co-workers.¹¹ The pressure buildup inside the particle is due to volume expansion of light gases and tars during coal devolatilization. The optimum value for the parameter P_{\min} in the CPD model was determined empirically from the tar yield data obtained in vacuum by Suuberg and co-workers.³² The predictions made using $P_{\min} = 0.01$ atm agree quite well with the reported total volatiles and tar yields for the bituminous coal for all ambient pressures.

The pressure dependence of the CPD model is due to the molecular weight of the finite fragments and the vapor pressure of each fragment. The choice of monomer mo-

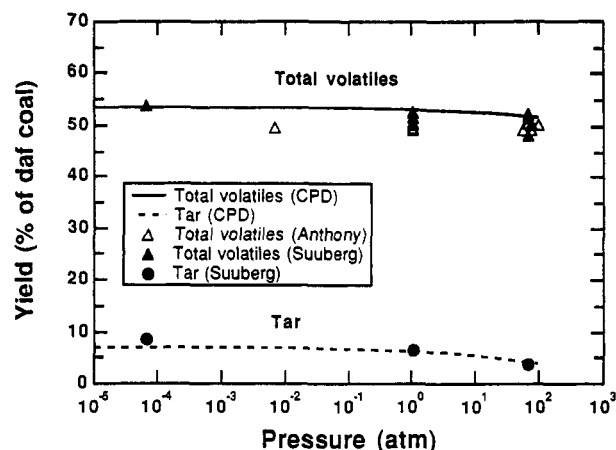


Figure 21. Comparison of CPD model predictions (curves) with pressure-dependent tar and total volatiles yield data (points) for a lignite.^{57,58}

lecular weight in any model is obviously coupled to the choice of vapor pressure coefficients, which means that curve-fitting these coefficients based on volatiles ultimate yield data does not provide a unique solution. In the CPD predictions shown, the input coefficients were determined from independent experiments (NMR and vapor pressure data). It was shown earlier that the Unger–Suuberg vapor pressure correlation²¹ gives higher boiling points than the FGP correlation (see Table I), especially at elevated pressures. CPD model show that the predicted yields using the two vapor pressure correlations are similar at atmospheric pressure and below, but that the predicted tar yield using the Unger–Suuberg correlation is lower than predicted by the FGP correlation at elevated pressures. For example, the CPD model predicted 3% tar yield at 100 atm with the Unger–Suuberg correlation and 11% with the FGP correlation. The fact that the FGP correlation was developed from vapor pressure and boiling point data of pure compounds, independently of tar yield data, is extremely encouraging.

CPD model predictions of the pressure-dependent devolatilization behavior of a lignite (using the FGP vapor pressure correlation) are shown in Figure 21, along with data from Anthony⁵⁷ and Suuberg.⁵⁸ The chemical structure coefficients used in these predictions were taken from a lignite, with adjustments in \mathcal{L}_0 and $f_{\text{gas},\infty}$ to match the tar and total volatiles yields at 1 atm. The tar yield for this lignite is very low, hence the small effect of pressure on total yield compared to the bituminous coal. Total volatiles yields for the lignite decrease only slightly with increasing pressure in both the experimental data and the model predictions. The predicted tar yield decreases slightly with increasing pressure, but the gas yield increases to compensate, and hence the slight decrease in total volatiles yield with increased pressure.

The lignite contains a large amount of mass in the side chains and bridges, as evidenced by the relatively high average bridge molecular weight ($m_b = 94$) used in the model. The number of aliphatic carbons per cluster determined by NMR analyses for lignites is twice that determined for bituminous coals.^{42,43} At atmospheric pressure, the gas precursors (side chains) attached to the tar are released as tar and can detach from the tar as light gas if the ambient gas temperature is high enough. In heated grid experiments, the gas is immediately quenched, and the gas precursors remain in the tar. At elevated pressures,

(57) Anthony, D. B. Sc.D. Thesis, Department of Chemical Engineering, Massachusetts Institute of Technology, 1974.

(58) Suuberg, E. M. Sc.D. Thesis, Department of Chemical Engineering, Massachusetts Institute of Technology, 1977.

more tar remains in the lignite, and the associated side chains are released as light gas. Due to the large mass in the side chains, the increased gas yield compensates for the decrease in tar yield.

Summary

The improved chemical percolation devolatilization (CPD) model discussed in this paper includes a realistic treatment of vapor-liquid equilibrium and a cross-linking mechanism. A new, generalized vapor pressure correlation for hydrocarbons such as tar and metaplast is proposed that is based on curve-fits of vapor pressure data from coal liquids. The new vapor pressure correlation compares well with pure component boiling points of hydrocarbons at pressures ranging from 0.007 to 10 atm and molecular weights ranging from 80 to 340 amu. This correlation is applicable to wider ranges of pressure, temperature, and molecular weight than previous generalized correlations that were based on limited experimental data. The use of a realistic vapor pressure expression eliminates much of the empiricism used to determine coefficients for devolatilization models.

The cross-linking mechanism used in the CPD model permits reattachment of metaplast to the infinite char matrix. The activation energy for the cross-linking rate is selected to be 65 kcal/mol based on comparisons of CPD model predictions with (i) measured total volatiles yields as a function of heating rate, (ii) pyridine extract data, and (iii) chemical structure data determined from NMR analyses of chars at different extents of devolatilization.

Coal-dependent input parameters for the CPD model are taken from chemical characteristics of the parent coal, wherever possible. Four of the five coal-dependent chemical structure parameters in the CPD model are taken directly from NMR analyses of the parent coal ($\sigma + 1$, M_{clust} , m_b , and p_0). This is a significant change in philosophy from previous treatments; these input parameters are fixed by the NMR analyses rather than used as fitting parameters. The fifth chemical structure parameter (c_0) is 0.0 for bituminous coals and is determined from measured tar yields for low- and high-rank coals. In low-rank coals, c_0 approximates the cross-linking that occurs prior to tar release at low heating rates, as evidenced by solvent-swelling analyses^{39,40} and by NMR analyses of lignites.⁴² In high-rank coals, such as low volatile bituminous coals, c_0 represents stable bridges, such as biaryl and aryl-ether linkages, which occur more frequently in the high-rank coals than in medium and low rank coals. Identical kinetic rate parameters are used for all coals.

Predictions of the amount and characteristics of tar from 16 different coals compare well with available data. Total yields predicted by the CPD model are also in good agreement with measured yields. The initial amounts of metaplast predicted by the CPD model for parent coals correlate roughly with 1-h extract yields in tetrahydrofuran, rather than extract yields in pyridine. Predicted tar molecular weights roughly agree with size-exclusion chromatography (SEC) data and field ionization mass spectrometry (FIMS) data with no adjustments of the input parameters or the vapor pressure correlation.

The model quantitatively predicts the observed decrease in tar and total volatiles yields for bituminous coals as pressure is increased in heated grid experiments with long hold times, using cluster molecular weights from NMR data and the new vapor pressure correlation. As the ambient pressure increases, the vapor pressure necessary for evaporation increases, and hence lower molecular weight fractions of the metaplast are released from the coal as tar vapor. Predictions of total volatiles yields from a lignite

show no increase with increasing pressure, as observed experimentally. The model shows that the lignite contains a large mass of bridge material compared to the bituminous coal and that the decrease in tar yield with increasing pressure is compensated by an increase in gas yield for the lignite.

The CPD model includes the principal thermochemical processes involved in coal pyrolysis. The fact that many of the characteristics of tars from different types of coals can be calculated from chemical structure data for the parent coal, without artificial adjustment of vapor pressure correlations or molecular weight distributions, is encouraging. It is hoped that additional chemical structure data for coal tars and chars can be used to refine the simple mechanisms currently used in the CPD model. Attention should also be focused on molecular weight distributions, as well as on the early cross-linking that occurs in low-rank coals.

Acknowledgment. Work supported by the U.S. Department of Energy's Pittsburgh Energy Technology Center's Direct Utilization AR&TD Program, the DOE Division of Engineering and Geosciences through the Office of Basic Energy Sciences, and by the National Science Foundation through the Advanced Combustion Engineering Research Center (ACERC) under Grant No. CDR-8522618 at Brigham Young University and the University of Utah. Discussions with Don Hardesty and Larry Baxter at Sandia are gratefully acknowledged.

Nomenclature

A	preexponential factor for rate constant
c	population of char bridges, on a per bridge basis
C_{clust}	number of carbons per aromatic cluster
E	activation energy for rate constant
f	mass fraction, function
f_a	percentage of aromatic carbon (carbon aromaticity)
f_i	moles of species i in feed stream
F_n	number of n -cluster finite fragments
F	moles of feed stream for flash distillation calculation
g_1	gas formed from side chains
g_2	gas formed from labile bridge stabilization to form char
k	kinetic rate coefficient
K_i	vapor-liquid equilibrium constant for species i ($K_i = y_i/x_i$)
l_i	moles of species i in liquid phase
L	moles of liquid phase for flash distillation calculation
\mathcal{L}	population of labile bridges, on a per bridge basis
m	mass
M	molecular weight
n	number of aromatic clusters per finite fragment (size bin)
p	population of intact bridges, on a per bridge basis ($p = \mathcal{L} + c$)
P	total pressure
P_i^v	vapor pressure of species i
Q_n	number of finite fragments on a per cluster basis ($Q_n = F_n/n$)
r_{ba}	ratio of mass of bridges to mass of aromatic material (m_b/m_a)
R	universal gas constant
t	time
T	temperature
v_i	moles of species i in vapor phase
V	moles of vapor phase in flash distillation calculation
x_C	mass fraction of carbon (daf basis)
x_i	mole fraction of species i in liquid phase
y_i	mole fraction of species i in gas phase
z_i	mole fraction of species i in feed stream
α	coefficient in vapor pressure correlation

β	coefficient in vapor pressure correlation	cross	cross-link
γ	coefficient in vapor pressure correlation	fin	finite fragment material (detached from infinite coal matrix)
δ	population of side chains	frag	fragment
ρ	composite rate coefficient ($\rho = k_c/k_b$)	gas	light gas
τ	number of broken bridges on the perimeter of a fragment	i	arbitrary species index
$\sigma + 1$	coordination number (number of attachments per cluster)	meta	metaplast
		tar	tar
		n	number of clusters per finite fragment (monomer, dimer, trimer, etc.)
		NMR	from nuclear magnetic resonance data on coal and char particles
		0	initial condition (parent coal)
		δ	side chains
		∞	final or infinite condition (fully pyrolyzed coal)

Subscripts

a	aromatic
b	bridge
C	carbon
clust	cluster

Aqueous High-Temperature Chemistry of Carbo- and Heterocycles. 17.¹ Thiophene, Tetrahydrothiophene, 2-Methylthiophene, 2,5-Dimethylthiophene, Benzo[*b*]thiophene, and Dibenzothiophene

Alan R. Katritzky* and Marudai Balasubramanian

Department of Chemistry, University of Florida, Gainesville, Florida 32611-2046

Michael Siskin*

Corporate Research Science Laboratory, Exxon Research and Engineering Company, Annandale, New Jersey 08801

Received January 21, 1992. Revised Manuscript Received May 4, 1992

The title compounds are unaffected under both thermolysis and neutral aquathermolysis conditions up to 350 °C. In the presence of 10% phosphoric acid, thiophene gave tetrahydrothiophene and 2-methylthiophene as major products along with other mono-, di-, and trimethylthiophenes, and di- and trithienyl derivatives as minor products. 2-Methylthiophene afforded 2,4- and 2,7-dimethylbenzothiophenes as major products in addition to di- and trithienyl derivatives. 2,5-Dimethylthiophene is very reactive and furnished several mono- and disubstituted methyl-, ethyl-, propyl-, and butylthiophenes in appreciable amounts. Benzothiophene gave several higher molecular weight products by desulfurization, by Diels-Alder reaction, and by dimerization processes. Tetrahydrothiophene and dibenzothiophene showed no reaction, even at 350 °C for 5 days with 10% phosphoric acid.

Introduction

Heavy oil contains up to 5 wt % of sulfur which is present as a variety of aliphatic and aromatic organosulfur compounds.² Steam stimulation of heavy oil reservoirs to improve oil mobility and recovery is now a well-established technique. This methodology³ brings the oil phase and host rock or sand into intimate contact with water at temperatures as high as 350 °C. At high temperature, steam can react directly to hydrolyze organosulfur compounds to produce H₂S, CO₂, hydrocarbon gases, and a complex array of secondary organosulfur compounds.^{1,4,5} Metals occurring naturally within the heavy oil and mineral matter of the host reservoir may play a role in the aquathermolysis of these compounds. Accelerated breakdown of the organosulfur compounds present in

heavy oil could simplify the overall oil structure and possibly reduce the oil viscosity.

Previous papers of this series have been concerned with the thermolysis and aquathermolysis of several classes of sulfur derivatives, specifically thioethers and disulfides,⁶ and of thiols and sulfonic acids.⁷ In a more recent publication, the generation of hydrogen sulfide from the various types of organosulfur compounds under aquathermolysis conditions was specifically discussed.¹ We now report the aquathermolysis chemistry of thiophene and several of its derivatives.

The gas chromatographic behavior of starting materials and products in this work is summarized in Table I. Table II records the source and mass spectral fragmentation of the authentic compounds used, either as starting material or for the identification of products. Tables III and IV record the mass spectral fragmentation patterns of products for which authentic samples were not available and

(1) Part 16: Katritzky, A. R.; Murugan, R.; Balasubramanian, M.; Greenhill, J. V.; Siskin, M.; Brons, G. *Energy Fuels* 1991, 5, 823.

(2) Clugston, D. M.; George, A. E.; Montgomery, D. S.; Smley, G. T.; Sawatzky, H. *Adv. Chem. Ser.* 1976, 151.

(3) Van Poolen, H. K., *Fundamentals of Enhanced Oil Recovery*; Penwell Publishing: Tulsa, OK, 1980.

(4) Clark, P. D.; Hyne, J. B.; Tyrer, J. D. *Fuel* 1983, 62, 959.

(5) Clark, P. D.; Hyne, J. B.; Tyrer, J. D. *Fuel* 1984, 63, 125.

(6) Katritzky, A. R.; Lapucha, A. R.; Greenhill, J. V.; Siskin, M. *Energy Fuels* 1990, 4, 562.

(7) Katritzky, A. R.; Lapucha, A. R.; Luxem, F. J.; Greenhill, J. V.; Siskin, M. *Energy Fuels* 1990, 4, 572.